NEA/NSC/DOC(95)03/IV
Volume IV

LEU-COMP-THERM-003

WATER-MODERATED U(2.35)O_2 FUEL RODS IN 1.684-CM SQUARE-PITCHED ARRAYS (GADOLINIUM WATER IMPURITY)

Evaluator

Virginia F. Dean
Idaho National Engineering Laboratory

Internal Reviewer
Carol A. Atkinson

Independent Reviewer

Nigel R. Smith
AEA Technology

ACKNOWLEDGMENTS

The author wishes to thank three of the experimenters, Sid Bierman, Duane Clayton, and Michael Durst, who provided much valuable additional information about how the experiments were conducted and reviewed the draft evaluation. She would also like to thank Roger Meade and Linda Sandoval of the Los Alamos National Laboratory Archives, who assisted in finding stored logbooks. Thanks also to Pam A. Thurman of Environmental Health Sciences of the Hanford Environmental Health Foundation, who found the worksheet verifying the Gd impurity data. And, thanks to Soon Sam Kim of Idaho National Engineering Laboratory, who assisted in completing calculations.

WATER-MODERATED U(2.35)O_2 FUEL RODS IN 1.684-CM SQUARE-PITCHED ARRAYS (GADOLINIUM WATER IMPURITY)

IDENTIFICATION NUMBER: LEU-COMP-THERM-003 SPECTRA

KEY WORDS: gadolinium, Gd, low enriched fuel rods, low enriched uranium, PNL, ^{235}U, uranium dioxide

1.0 DETAILED DESCRIPTION

1.1 Overview of Experiment

A series of critical approach experiments with clusters of aluminum clad U(2.35)O_2 fuel rods in a large water-filled tank was performed over the course of several years at the Critical Mass Laboratory at the Pacific Northwest Laboratories (PNL). Experiments included rectangular, square-pitched lattice clusters, with pitches of 2.032 cm (LEU-COMP-THERM-001) or 1.684 cm. Some of these experiments were performed with absorber plates of various materials between clusters (LEU-COMP-THERM-016). Others added reflecting walls of depleted uranium, lead, and steel on two opposite sides of the cluster array (LEU-COMP-THERM-017). Some circular, triangular-pitched lattices, with pitches of 1.598 cm or 1.895 cm, were used to measure the effect of gadolinium dissolved in the water (LEU-COMP-THERM-005).

This evaluation documents water-reflected clusters at 1.684-cm pitch with no absorber plates, reflecting walls, or large amounts of dissolved poison. However, a small amount of gadolinium impurity in the water was reported. A total of 23 experiments were evaluated. All of these were judged to be acceptable as benchmark data.

Information in this section comes from References 1-10, which are the original PNL reports of these experiments. References 4, 5, and 6 are the primary references for this particular set of experiments. References 11-15 provide supplementary information. Details which are from specific references are so noted.

1.2 Description of Experimental Configuration

1.2.1 Experiment Tank and Surroundings - Experiments were performed in a 0.952-cm-thick, open-top, carbon-steel tank. Tank inside dimensions were 1.8 x 3.0 x 2.1 meters deep. The experiment was centered in the tank to within one-quarter inch.

The control blade, the safety blade, and any control or safety rods were withdrawn above the top water reflector for the reported configurations. Other than radiation detectors and support structures (acrylic support plate, acrylic or polyethylene lattice plates, 6061 aluminum angle supports, and control/safety blade guides are all described in this section), no other apparatus was in the tank.[a] (See Figures 1 and 2.)

[a] Tank dimensions were from References 1-10. Other information was from private communication, Sid Bierman, July 1993.

Figure 1. Experiment Tank.

Figure 2. Arranging Fuel Rods.

The experiment tank was located in one corner of the Critical Mass Laboratory at the Pacific Northwest Laboratories, Hanford, Washington. The tank sat upon a concrete floor, which was at least 40.6 cm thick (Reference 11, p. 32). The concrete walls of the room were 5 feet thick. The concrete ceiling was 2 feet thick and approximately 20 feet high. The tank was located approximately four feet from the two closest corner walls.[a]

1.2.2 Fuel Rod Support Plate - The bottoms of the fuel rods were supported by a 2.54-cm-thick, acrylic support plate. In the 1-, 2-, and 3-cluster experiments, the width and length of the support plate were approximately the width and length of the clusters. The acrylic support plate was supported by two 15.3 x 5.08 x 0.635 cm 6061 aluminum channels oriented so that the bottom surface of the support plate

[a] Sid Bierman, private communication, July 1993.

was 15.3 cm above the bottom of the tank. For the 4-cluster experiments, the support plate extended nearly the length and width of the tank and was supported by 6061 aluminum angles attached to the tank walls.[a]

1.2.3 Lattice Plates and Supports - The pitch of the fuel rods was maintained by two levels of polypropylene lattice plates. Holes for the fuel rods were no more than 5 mils (0.0127 cm) larger than the rod diameter.[b]

The top lattice plates were bolted to 5.08 x 5.08 x 0.635 cm aluminum angles, attached at their ends to the walls of the tank. In one experiment, these aluminum lattice supports were doubled, with no effect on the critical separation between clusters (Reference 1, pp. 26 and 28). The bottom lattice plates rested on the fuel rod support plate. The bottom surface of the top lattice plates was approximately 77.7 cm above the fuel rod support plate.[c]

In some 3-cluster experiments, the required horizontal separation between bottom lattice plates or between bottom lattice plates and the control/safety blade guides, was maintained by shims. This was necessary in order to position the bottom lattice plates accurately. (The control and safety blade guides could not, by themselves, be used for positioning since they were not fastened to anything below their attachment to the angles supporting the top lattice plates.) The shim was either Lucite or was made from the lattice plate material. The Lucite shim was approximately 1 inch thick.[d]

1.2.4 Radiation Detectors - The boron-lined proportional counters (usually three in number) were placed symmetrically around the experiments. The detectors were kept dry by being placed in aluminum tubes that extended above the top surface of the water. The elevation of the detectors varied, depending on the buoyancy of the tube holding the detector. The aluminum tubes were approximately 1.5 inches in diameter and were placed about 30 cm from the experimental assembly, always outside a 15-cm thickness of water.[e]

---

[a] Sid Bierman recalls that there may have been three separate support plates for the 3-cluster experiments. Exact dimensions of the support plates are not known. (Private communication, Sid Bierman, August 1993.)

[b] Sid Bierman, private communication, August 1993.

[c] Reference 4, pp. 11 and 20.

[d] Private communication, Sid Bierman, August 1993.

[e] Private communication, Sid Bierman, July 1993.

1.2.5 Water Reflector - The top water surface was always at least 15 centimeters above the top of the fuel region of the rods. (Reference 14, p. 132)[a] The bottom water reflector also was at least 15 centimeters thick, since the aluminum angle supporting the fuel-rod support plate above the bottom of the tank was 15.3 cm high. The minimum side-reflector thickness, assuming that the experiment was centered in the tank and that the longer side of the experiment parallelled the longer side of the tank, was ~59 centimeters.[b]

1.2.6 Others - A ^{252}Cf source of approximately 0.6 micrograms was placed near the center of each experimental assembly. The source was mounted in an open acrylic tube, 0.6 cm in diameter (Reference 8, p 2.3) and two or three inches long.[c] During the triangular-pitched experiments, no measurable effect on critical size was detected with replacement-type reactivity worth measurements of the californium source (Reference 8, pp. 3.6 and 3.7).

The aluminum control and safety blade guides, were located between clusters in multi-cluster experiments. The blade guides, two for the control blade and two for the safety blade, extended from the bottom of the fuel pin array to well above the water surface. Two slightly different sizes of guides were used throughout the series of experiments. All guides were 3.8 cm wide and were either 2.54 cm thick (Reference 3, p. 5) or 1.27 cm thick (Reference 4, p. 27), with a slot for the blades that was either 0.96 cm wide or 0.64 cm wide.[d] During one experiment from the first set of experiments, an extra thickness of aluminum was added to the control and safety blade guides. The results demonstrated "no change in the predicted critical separation between fuel rod clusters." (Reference 1, pp. 13 and 28)

1.2.7 Fuel Rods - Fuel rod dimensions are given in diagrams in References 1, 3-6, and 8. These diagrams are the same as Figure 3, which is a reproduction of an annotated diagram from Reference 13 (Vol 1, p. 29). Reference 13 is cited by Reference 8, p. 2.7, as the source of fuel rod data.

---

[a] Confirmed by private communication, Sid Bierman, July 1994.

[b] Case 12. See Figure 6.

[c] Private communication, Sid Bierman, August 1993.

[d] Different widths of control and safety blades were used for different experiments. (Private communication, Sid Bierman, August 1993.)

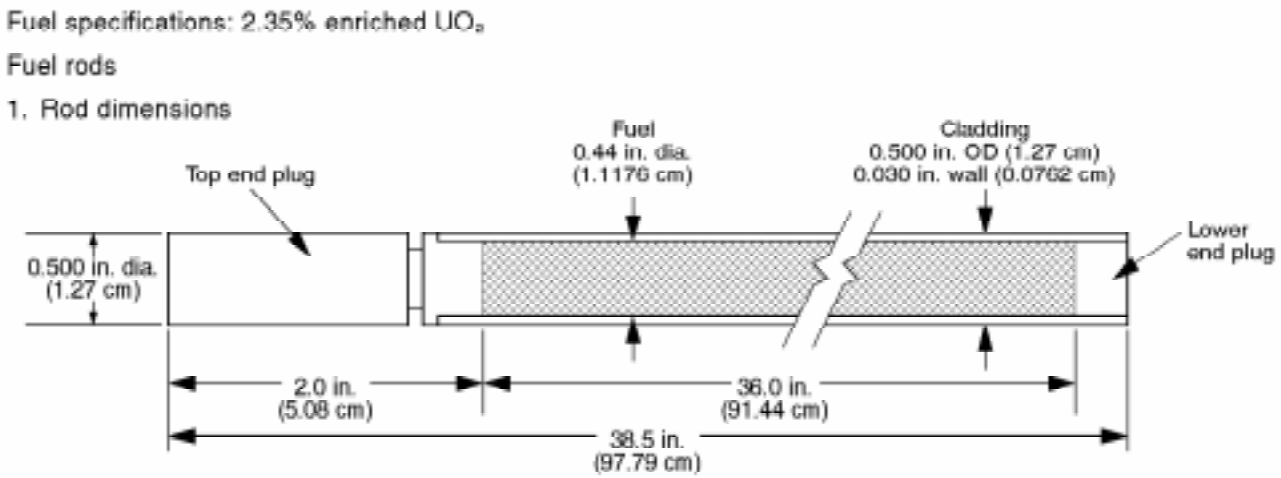

Figure 3. U(2.35)O_2 Fuel Rod.

Dimensions of the U(2.35)O_2 fuel rods are summarized in Table 1.

Table 1. 2.35 Wt.% Enriched UO_2 Fuel Rod Dimensions.

Component	Length (cm)	Diameter (cm)
UO_2 fuel	91.44	1.1176
Top end plug (1100 Al)	5.080	1.27
Lower end plug (5052-H32 Al)	1.27	1.1176
Clad (6061 Al)	~93.19[(a)]	1.270 OD (.0762 cm thick)

(a) This length is an approximation based on measuring Figure B-1 in Reference 13 (Vol. 1, p. 29). Total rod length is 97.79 cm. The clad envelops the lower end plug, fuel, and ~0.48 cm of the top end plug. Dimensions of the notch shown in the top end plug are not known.

1.2.8 Experimental Method for Determining Critical Configuration[a] - The critical configuration was determined by measuring neutron detector count rates (above background) produced by subcritical configurations and extrapolating to the critical condition. In particular, the averages of several (usually four, five, or six) 80-second counts from each of two or three detectors were recorded for at least two loading configurations. For single cluster experiments or those with clusters positioned at predetermined separation distances, a plot of [number of fuel rods]/[count rate] vs. [number of fuel rods] was linearly extrapolated to zero to determine the critical number of rods predicted by each detector. Then the results from the two or three detectors were averaged. Additionally, a plot of [1]/[count rate] vs. [number of fuel rods] was extrapolated to zero for each detector and the results averaged. Then the average critical number of fuel rods from these two averages was used as the final result.

For multiple clusters of predetermined sizes with varying separation distance between them, the same procedure was followed except that the variables plotted were [separation distance]/[count rate] vs. [cluster separation] and [1]/[count rate] vs. [cluster separation]. The final result was the average cluster separation distance.[b]

To vary the number of fuel rods or cluster separation, fuel rods were moved in half-row or whole-row increments. An example of half-row increment moves for varying cluster separation is shown in Figure 4 for three 15-by-8-rod clusters. For the four configurations represented in this example, the numbers of empty rows between clusters are 2, 1¾, 1½, and 1¼. The initial configuration is shaded. The separation distance resulting from each of the three moves is determined by multiplying the number of empty rows between clusters by the pitch and adding the constant separation distance between lattice plates, required for the control and safety blade guides.[c]

---

[a] This information is from study of the logbooks, which are stored at the Los Alamos National Laboratory Archives. See Appendix B for correlation between case number in this evaluation and experiment number under which experiment is stored at the archives.

[b] Plots of both [number of rods]/[count rate] vs. [number of rods] and [1]/[count rate] vs. [number of rods] (or [separation]/[count rate] vs. [separation] and 1/[count rate] vs. [separation]) were used because one tended to overestimate the critical number of rods and the other to underestimate it. The lower critical number prediction was used in applying the operational safety rule that no more than 85% of the difference between latest loading and predicted critical loading could be added. As criticality was approached, both curves tended to predict the same critical number of rods. (Private communication, Duane Clayton, August 1993.)

[c] Final rod additions were in half- or whole-row increments, so that the average rod worth of the addition was equal to the average rod worth of an entire row. Then, in computational models that homogenize the fuel rod cell, partial rows can be represented as a fraction of a fuel rod across the entire width of the cluster.

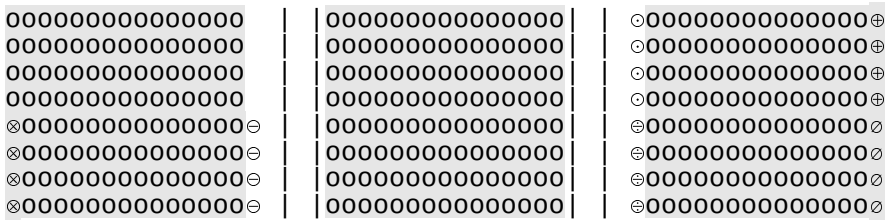

| | are safety and control blade guide widths
Initial load is shaded.
⊕ → ⊙ first move (1¾)[(a)]
⊗ → ⊖ second move (1½)[(a)]
⌀ → ⊜ third move (1¼)[(a)]

(a) This refers to the resulting average rows of separation between lateral clusters and central cluster after the stated move. Separation distance is then {[average rows of separation] x [pitch]} + [width of safety and control blade guides].

Figure 4. Method of Varying Separation Distances Between Clusters.

1.2.9 Critical Cluster Dimensions and Separations - Cluster sizes and separations for the 23 critical configurations are listed in Table 2 and are diagramed in Figures 5-8. Because the critical configuration was determined by extrapolation to critical, the critical number of rods was, in general, not an integral number. Placement of the twenty-five water holes, aluminum clad voids, or water-filled aluminum tubes of Cases 6-8 is shown in Figure 9.

Table 2. $U(2.35)O_2$ Fuel Rod Critical Configurations (See Figures 5-8).

Case Number	Number of Clusters	Cluster Dimensions (number of rods)[a] (X x Y)	Separation Between Clusters (cm)[b]	Reference (pg)
1	1	17 x 36.14[c] ± .012 (614.4 ± 0.2 rods total)	-	4 (12)
2	1	21 x 25.205[c] ± .005 (529.3 ± 0.1 rods total)	-	4 (12)
3	1	23 x 22.78[c] ± .017 (523.9 ± 0.4 rods total)	-	4 (12, 17)
4	1	24 x 21.8875[c] ± .008 (525.3 ± 0.2 rods total)	-	4 (12)
5	1	34 x 17.512[c] ± .003 (595.4 ± 0.1 rods total)	-	4 (12, 40)
6	1	23 x 22.209[c][d] ± .009 (485.8 ± 0.2 rods total)	-	4 (17)
7	1	23 x 23.861[c][e] ± .009 (523.8 ± 0.2 fuel rods total)	-	4 (17)
8	1	23 x 23.061[c][f] ± .009 (505.4 ± 0.2 fuel rods total)	-	4 (17)
9	4	17 x 17 (two lower) 17 x 0.647[c] ± .003 (two upper) (600.0 ± 0.1 rods total)	2.59 ± 0.08 (x- and y-separation)	4 (40)
10	2	17 x 17.265[c] ± .029 (587 ± 1 rods total)	1.68 ± 0.02 (x-separation)	4 (40)
11	4	17 x 17 (two lower) 17 x 3.859[c] ± .012 (two upper) (709.2 ± 0.4 rods total)	4.27 ± 0.08 (x- and y-separation)	4 (40)
12	4	17 x 17 (two lower) 17 x 15.115[c] ± .006 (two upper) (1091.9 ± 0.2 rods total)	5.95 ± 0.08 (x- and y-separation)	4 (40)
13	4	17 x 17 (two lower) 17 x 1 (two upper) (612 rods total)	2.59 ± 0.08 (x-separation) 5.11 ± 0.02 (y-separation)	4 (40)
14	4	17 x 17 (two lower) 17 x 2 (two upper) (646 rods total)	2.59 ± 0.08 (x-separation) 6.66 ± 0.02 (y-separation)	4 (40)
15	4	17 x 17 (two lower) 17 x 4 (two upper) (714 rods total)	2.59 ± 0.08 (x-separation) 7.53 ± 0.02 (y-separation)	4 (40)

Case Number	Number of Clusters	Cluster Dimensions (number of rods)[a] (X x Y)	Separation Between Clusters (cm)[b]	Reference (pg)
16	4	17 x 17 (two lower) 17 x 9 (two upper) (884 rods total)	2.59 ± 0.08 (x-separation) 9.00 ± 0.03 (y-separation)	4 (40)
17	4	17 x 17 (two lower) 17 x 12 (two upper) (986 rods total)	2.59 ± 0.08 (x-separation) 9.97 ± 0.02 (y-separation)	4 (40)
18	4	17 x 17 (two lower) 17 x 15 (two upper) (1088 rods total)	2.59 ± 0.08 (x-separation) 11.45 ± 0.03 (y-separation)	4 (40)
19	4	17 x 17 (all four) (1156 rods total)	2.59 ± 0.08 (x-separation) 13.87 ± 0.04 (y-separation)	4 (40)
20	3	25 x 20 (center) 17 x 20 (two outer)	9.88 ± 0.03	4 (41)
21	3	25 x 18 (center) 20 x 18 (two outer)	6.78 ± 0.02	4 (41) 6 (13)
22	3	25 x 18 (center) 20 x 18 (two outer)	6.826[g] ± 0.02	5 (15) 6 (13)
23	3	23 x 18 (center) 20 x 18 (two outer)	6.176 ± 0.02	6 (13)

(a) For two- or three-cluster configurations, the first dimension is along the direction of cluster placement. Second dimension is the width of facing sides, as shown in Figures 5-8.
(b) Distance between outer fuel-rod cell boundaries of clusters.
(c) This dimension is derived from total number of rods and the lattice width.
(d) Includes 25 "water holes" where water replaced fuel rods in the lattice. See Figures 5 and 9.
(e) Includes 25 "aluminum clad voids" where air-filled aluminum tubes, of the same diameter and length as the fuel rods, replaced fuel rods in the lattice. See Figures 5 and 9.
(f) Includes 25 "water-filled aluminum tubes" where aluminum tubes, of the same outer diameter and length as the fuel rods, filled with water, replaced fuel rods in the lattice. See Figures 5 and 9.
(g) Reference 5 gives the rod-surface-to-rod-surface separation between clusters as 7.24 cm. To obtain the separation between cell boundaries, subtract [pitch-rod diameter]. There is no gadolinium impurity in the water from this reference.

1.3 Description of Material Data

1.3.1 UO_2 Fuel - Figure 3 (from Reference 13, Vol. 1, p. 29) and results of a fuel rod sample analysis (Reference 13, Vol. 2, p. 3) are the basis for the fuel material characterization. A fuel rod contains 825 g of UO_2 powder, 726 g of 2.35 wt.%

enriched uranium, and 17.08 g of ^{235}U, at an oxide density of 9.20 g/cm^3.[a] The isotopic content of the uranium is given in Table 3.

Table 3. Isotopic Composition of Uranium in 2.35% Enriched UO_2 Fuel Rods (Reference 8, pp. 2.7 and 2.8).

Uranium isotope	Wt.%[(a)]
U-234	0.0137 ± .0007
U-235	2.350 ± .01
U-236	0.0171 ± .0007
U-238	97.62

(a) Values are originally from Reference 13, Vol 2, p. 3. Uncertainties are 3σ. Note that the total of all weight percents is 100.008.

1.3.2 Aluminum Alloys - Aluminum components of the fuel rods are the top (longer) end plug of 1100 aluminum, the lower end plug of 5052 aluminum, and the clad of 6061 aluminum. Measured densities and ASTM Standard chemical compositions of these three types of aluminum are given in Table 4.[b] The ASTM Standard for these three aluminum alloys includes limits on impurities to maximums of 0.05 wt.% each and 0.15 wt.% total.

Experiment support structures, including lattice plate supports and spacer rods, control/safety blade guides, tubes housing the proportional counters, and sleeves for gadolinium control rods, were 6061 aluminum alloy. The experimenters noted that doubling the amount of the aluminum angles supporting the grid plates in one experiment (Reference 1, p. 26) and the control and safety blade guides in another (Reference 1, p. 13) "resulted in no change in the predicted critical separation between fuel rod clusters." (Reference 1, p. 28).

[a] These values are not self-consistent. See discussion in Section 2.1.

[b] From Reference 8, pp. A.2-A.4, and from *Alcoa Aluminum Handbook*, Aluminum Company of America, pp. 46-50, 1967.

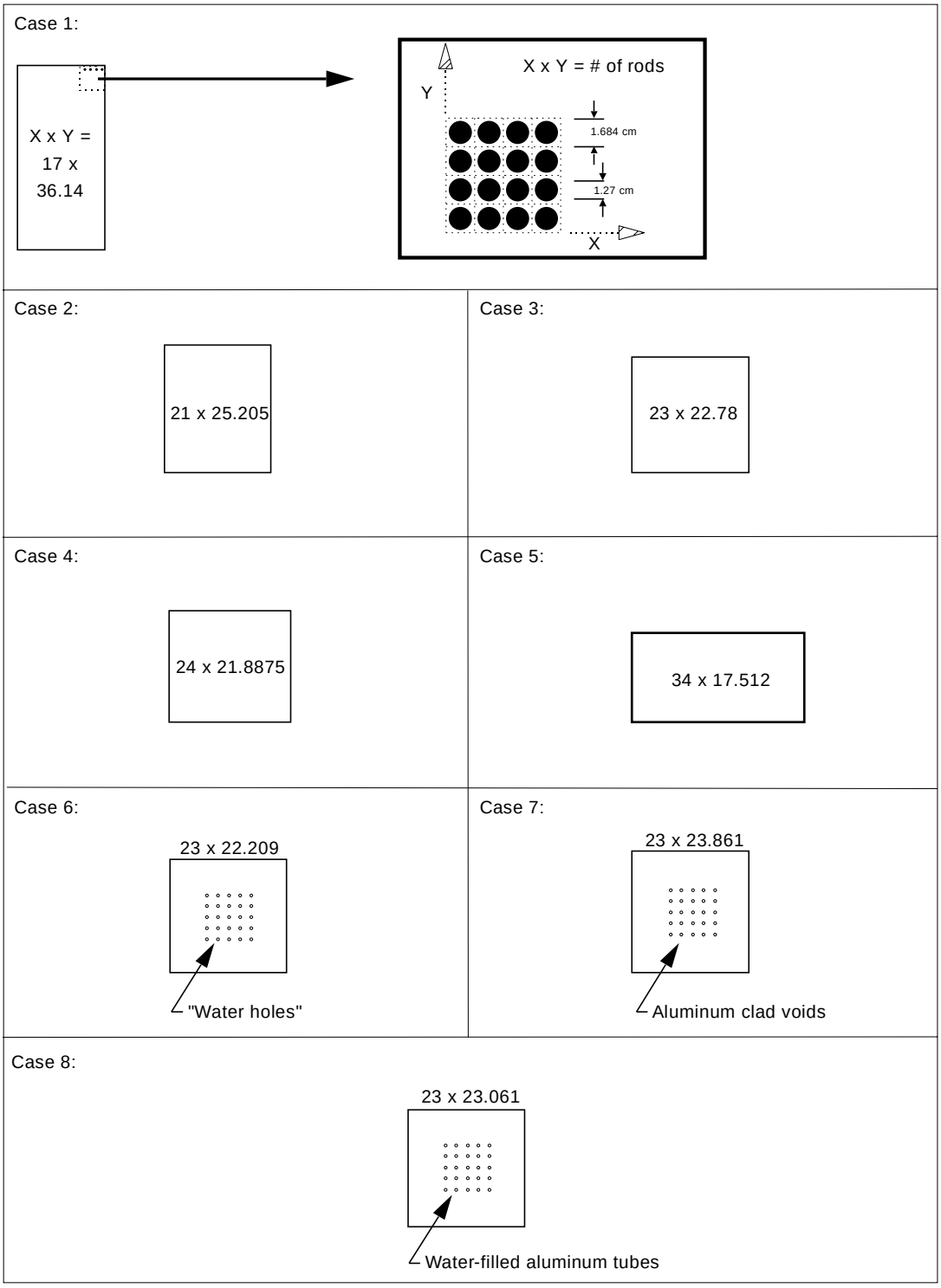

Figure 5. Critical Configurations of $U(2.35)O_2$ Fuel Rods at 1.684 Centimeter Pitch (Cases 1-8).

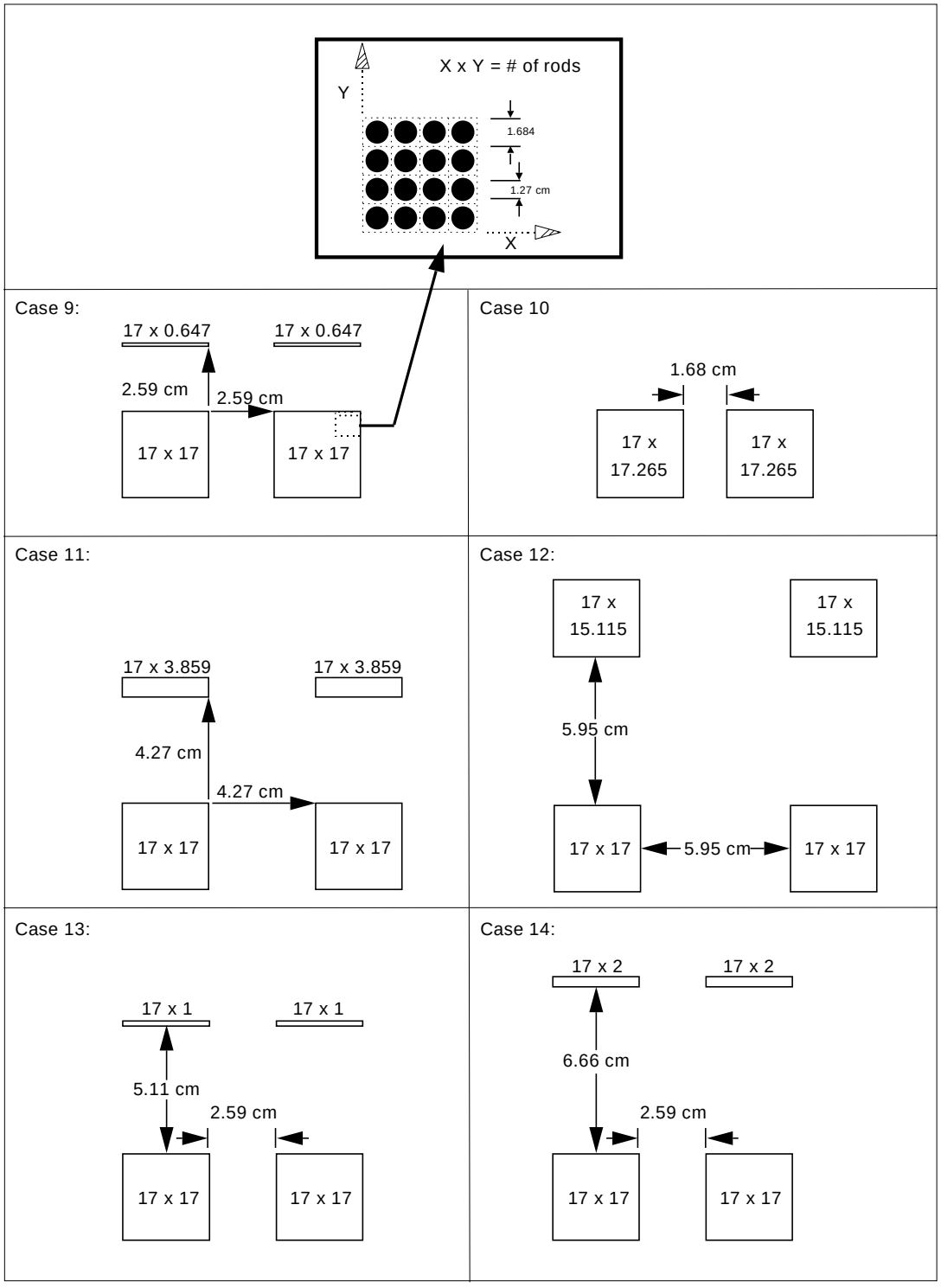

Figure 6. Critical Configurations of $U(2.35)O_2$ Fuel Rods at 1.684 Centimeter Pitch (Cases 9-14).

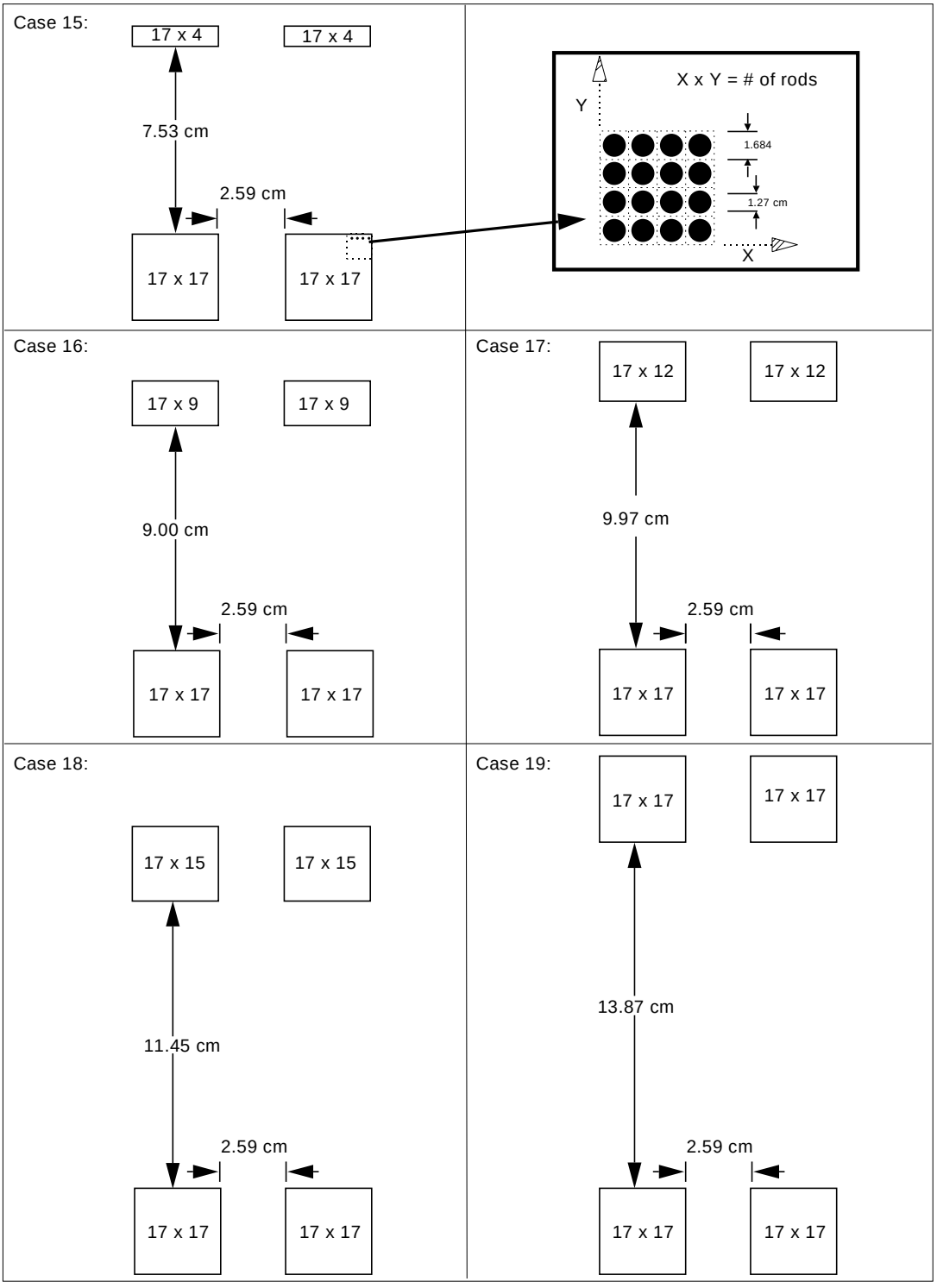

Figure 7. Critical Configurations of $U(2.35)O_2$ Fuel Rods at 1.684 Centimeter Pitch (Cases 15-19).

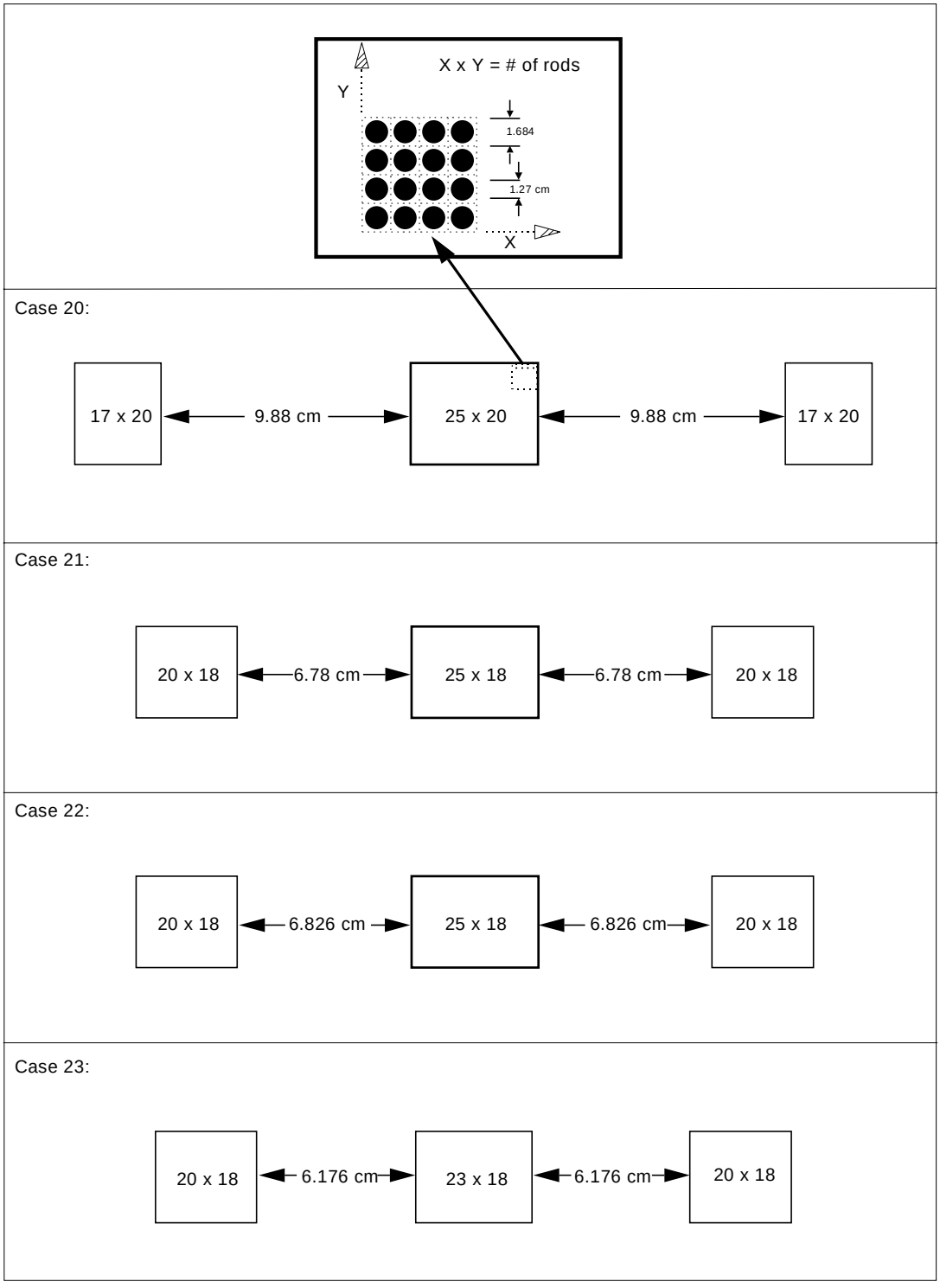

Figure 8. Critical Configurations of $U(2.35)O_2$ Fuel Rods at 1.684 Centimeter Pitch (Cases 20-23).

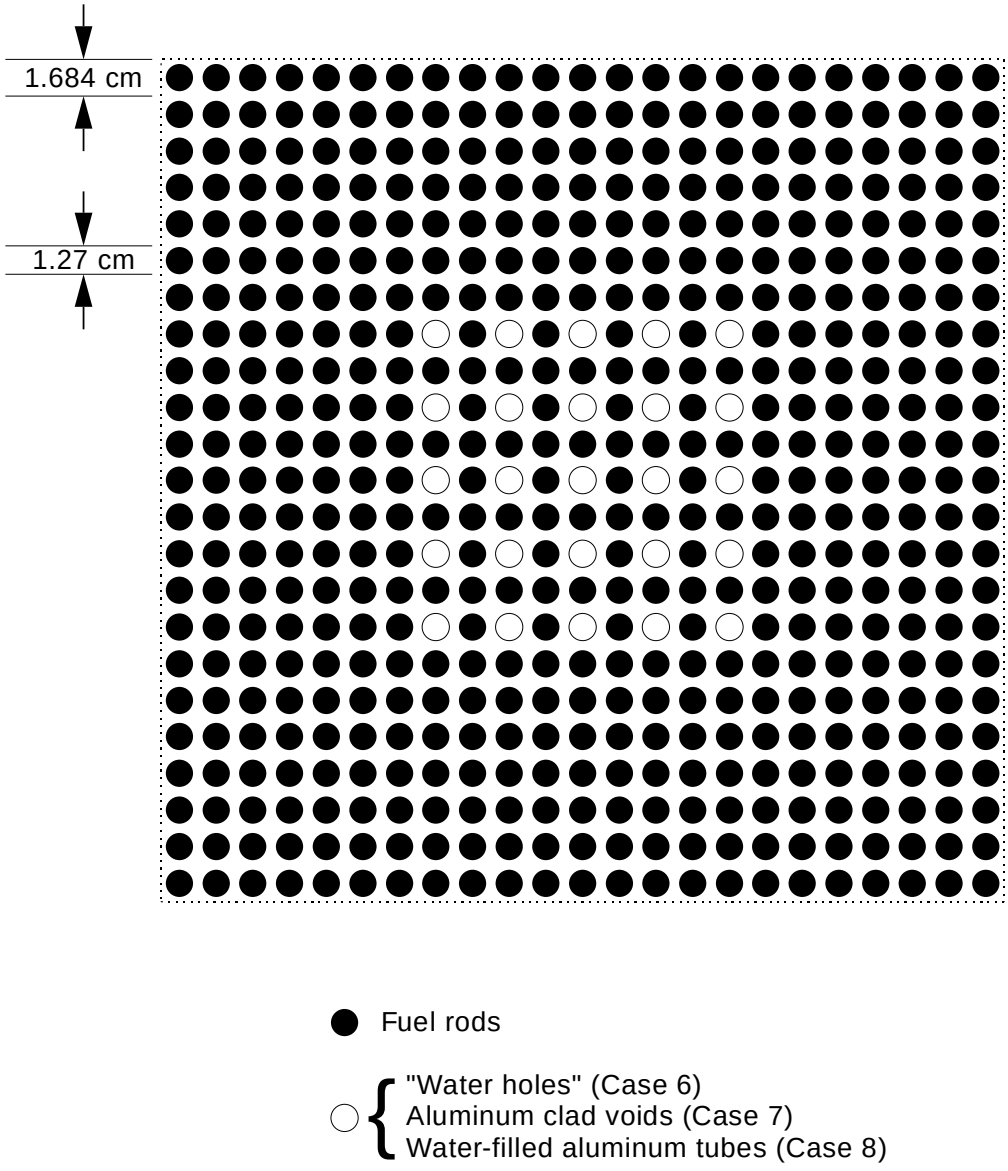

Figure 9. 23 x 23 Array of $U(2.35)O_2$ Fuel Rods at 1.684 Centimeter Pitch Showing Placement of Water Holes, Aluminum Clad Voids, and Water-Filled Aluminum Tubes (Cases 6-8).

Table 4. Measured Densities and Standard Compositions of Aluminum Alloys.

Element	Wt.%
1100 Aluminum (density - 2.70 g/cm^3)	
Si	1.0 (combined maximum)
Fe	
Cu	0.05-0.20 (0.12 nominal)
Mn	0.05 (maximum)
Zn	0.10 (maximum)
Al	99.00 (minimum)
5052 Aluminum (density - 2.69 g/cm^3)	
Si	0.45 (combined maximum)
Fe	
Cu	0.10 (maximum)
Mn	0.10 (maximum)
Mg	2.2-2.8 (2.5 nominal)
Cr	0.15-0.35 (0.25 nominal)
Zn	0.10 (maximum)
Al	remainder (96.10-97.65)
6061 Aluminum (density - 2.69 g/cm^3)	
Si	0.40-0.80 (0.6 nominal)
Fe	0.7 (maximum)
Cu	0.15-0.40 (0.25 nominal)
Mn	0.15 (maximum)
Mg	0.8-1.2 (1.0 nominal)
Cr	0.04-0.35 (0.2 nominal)
Zn	0.25 (maximum)
Ti	0.15 (maximum)
Al	remainder (96.00-98.61)

1.3.3 Water - Laboratory analyses of the water in the tank were done. The reported impurity concentrations are given in Table C.1 of Appendix C. The approximate average water temperature was 22°C.[a] This corresponds to a density of 0.997766 g/cm^3.[b]

The conclusion of the evaluations of the water impurity analyses in Appendix C and in Section 2.3 is that the gadolinium impurity reported in Reference 4 is significant. No gadolinium impurity is reported in Reference 5. Therefore, the configuration described in Reference 6 as the average of two previously reported experiments (from References 4 and 5) is considered in this evaluation to be two separate configurations, Cases 21 and 22.

1.3.4 Lattice Plates and Fuel Rod Support Plates - The acrylic fuel rod support plates had a density of 1.185 g/cm^3 and were 8 wt.% hydrogen, 60 wt.% carbon, and 32 wt.% oxygen. (Reference 4, pp. 11 and 20; Reference 14, p. 133) Uncertainties and methods of determination were not given.

The polypropylene (C_3H_6) lattice plates had a density of 0.904 g/cm^3. (Reference 4, pp. 11 and 20; Reference 6, p. 3; Reference 14, p. 133)

1.3.5 Tank - The experiment tank was carbon steel, which is approximately 1 wt.% Mn, 0.9 wt.% C, and the remainder, 98.1 wt.%, Fe.[c]

[a] Estimated from occasional logbook values.

[b] Interpolated between densities at 20 and 25°C, CRC Handbook of Chemistry and Physics, 68th Edition, p. F-10.

[c] Robert C. Weast, ed., *CRC Handbook of Chemistry and Physics, 68th Edition*, CRC Press, p. E-114, 1987.

2.0 EVALUATION OF EXPERIMENTAL DATA

Experiments were well documented and carefully performed. There were no significant omissions of data.

2.1 Fuel Rod Data

Some uncertainty exists in the characterization of the fuel rods. Dimensions and masses are stated in the source document (Reference 13, Vol. 1, p. 29) with no mention of measurement techniques or uncertainties. The 3σ-uncertainty in enrichment is stated as 0.01 wt.% without further discussion (Reference 13, Vol. 2, p. 3).

As was mentioned in Section 1.3, quantities characterizing the mass of fuel are not self-consistent. Table 5 gives the mass of ^{235}U derived in different ways from the given quantities. The highest and lowest masses represent a difference in uranium mass of less than 0.2% (726 g vs. 727.22 g).

Table 5. Mass of ^{235}U Per $U(2.35)O_2$ Fuel Rod Derived from Different Sets of Given Quantities.

U-235 mass derived from the following given quantities:	U-235 Mass (g)
U-235 mass[(a)]	17.08
Mass of U (726 g)[(b)] and 2.35 wt.% ^{235}U	17.0610
Mass of UO_2 (825 g)[(c)] and 2.07 wt.% ^{235}U in UO_2 [(d)]	17.0775[(e)]
UO_2 density (9.20 g/cm^3)[(c)], volume of fuel[(f)], and 2.07 wt.% ^{235}U in UO_2 [(d)]	17.0827
Mass of UO_2 (825 g)[(c)], 2.35 wt.% ^{235}U, and 2-to-1 ratio of O atoms to U atoms in UO_2	17.0896
Total rod mass (917 g)[(a)], volume[(f)] and density of aluminum, and 2.07 wt.% ^{235}U in UO_2 [(d)]	17.0775

(a) Given only in Reference 1.
(b) Given in References 1 and 8.
(c) Given in all reports on experiments with 2.35 wt.% enriched rods. (References 1, 3-6, and 8.)
(d) Reference 13, Vol. 2, p. 3.
(e) Using this mass and the given wt.%'s of the uranium isotopes gives a formula for uranium dioxide of $UO_{2.012}$. This is within the typical range for UO_2 powders of $UO_{2.005}$ and $UO_{2.129}$.[a]
(f) Calculated from reported dimensions.

The magnitudes of other uncertainties in fuel rod data are taken as half the value of the least significant digit, when the uncertainty is not given. The effects on k_{eff} of the uncertainties in enrichment, fuel diameter, fuel length, clad

[a] C. R. Tipton, Jr., ed., *Reactor Handbook, Second Edition*, Interscience Publishers, Inc., N.Y., Vol. I, p. 292.

thickness, pitch, and uranium mass for a near-critical configuration are summarized in Table 6. The last two entries are the calculated results from two models that contain a combination of individual changes. Results indicate that effects on k_{eff} due to uncertainties in fuel rod characterization and pitch could be as great as 0.25%. Note that this is for the case of all rods having all changes that affect k_{eff} positively, which is unlikely. Also, the uncertainty in pitch is itself especially conservative. (See footnote c of Table 6.) However, an uncertainty of ±0.25% due to uncertainties in fuel rod characterization may be included in the benchmark-model k_{eff}.

Table 6. Sensitivity of k_{eff} to Uncertainties in Fuel Rod Characterization.

Quantity (Amount of Change)	% Δk_{eff} (ONEDANT)[(a)] for Increase in the Quantity	% Δk_{eff} (ONEDANT)[(a)] for Decrease in the Quantity
Enrichment (± 0.01 wt.%[(b)])	+0.08	-0.13
Fuel Diameter (± 0.0127 cm)	+0.03	-0.02
Fuel Length (± 0.127 cm)	+0.02	-0.02
Clad Diameter (± 0.00127 cm)	+0.01	+0.02
Pitch (± 0.0076 cm[(c)])	+0.08	-0.09
Uranium Mass (-0.81 g and +0.41 g)	-0.01	-0.01
All above changes that individually increase k_{eff}	Δk_{eff} = +0.25%	
All above changes that individually decrease k_{eff}	Δk_{eff} = -0.20%	

(a) 27-group cross sections with homogenized lattice-cell fuel region (CSASIX); sample input given in Appendix D.
(b) 3σ uncertainty (Reference 13, Vol. 2, p. 3)
(c) The largest standard deviation for sets of center-to-center spacing measurements for triangular pitch lattice plates of Reference 8 (Appendix E) was 0.003 inch (0.0076 cm). References 7 (p. 2) and 8 (p. 36) give the uncertainty in pitch as ± 0.005 cm. References 9 (p. 3.2) and 10 (Appendix D) give the uncertainty in pitch as ± .001 cm.

2.2 Reflector Thickness

2.2.1 Top Water Reflector - The minimum thickness of the top water reflector is 15 cm above the fuel region. Since the top end plug is 2 inches (5.08 cm) long, the minimum water reflector thickness above the rods is 9.92 cm.

Calculations were performed for a an infinite-slab fuel region with a water reflector on both sides. ONEDANT and 27-group cross sections, with a lattice-cell fuel region homogenized by XSDRNPM, were used. The reflector thickness was varied from 15 to 30 centimeters. The effect on k_{eff} of the outermost 15 centimeters of water was less than 0.002%. Replacing the outermost 15 centimeters of water with 40 centimeters of full-density stainless steel or concrete gave similar results: the effect on k_{eff} was less than 0.004%.

These calculations indicate that a top water reflector with a thickness of 15 centimeters may be considered as "effectively infinite," and the effects of materials beyond the top and bottom reflectors may be neglected. Therefore, the lack of data about material above the 15-cm-thick top water reflector does not affect the acceptability of these experiments as benchmark critical experiments.

2.2.2 Side Water Reflector - Additionally, ONEDANT was used to determine the effect of radial-reflector thickness for a near-critical, cylindrical, XSDRN-homogenized array of pins. The difference in k_{eff} between a 15-cm-thick side reflector and a 30-cm-thick side reflector is 0.01%. Replacing the outermost 15 centimeters of the 30-cm-thick water reflector with 20% stainless steel in water affects k_{eff} by less than 0.002%. Therefore, lack of specifications about detectors, which were placed in the water reflector more than 15 centimeters away from the clusters, does not affect the acceptability of these experiments.

2.3 Gadolinium Impurity

Water impurity sensitivity studies in Appendix C and Section 3.3.2 indicate that the only significant impurity is the gadolinium impurity reported in Reference 4. For Cases 1-21, from Reference 4, a gadolinium concentration of 10.4 ± 3.6 g/m^3 is reported to be present in the water moderator and reflector. However, no gadolinium impurity is reported in References 5 and 6 (Cases 22 and 23).

One experimenter[a] provided the results of the water sample analyses for experiments reported in Reference 4. A letter from Loren J. Maas of the Hanford Environmental Health Foundation to B. M. Durst dated August 31, 1979, stated the results of analyses of three water samples from the set of experiments from Reference 4. The gadolinium results were stated in the letter as 12.0, 6.3, and

[a] Private communication, Sid Bierman, September 1993.

13.0 mg/liter of Gd. The average value is 10.4 g/m^3 with a standard deviation of 3.6 g/m^3, as reported in Reference 4. The three Gd sample values were verified by P. A. Thurman of the water analysis laboratory, who checked the original laboratory worksheet. Recorded values were 12.3, 6.3, and 12.6 mg/l of gadolinium. (Apparently these values were rounded to two significant figures in the letter reporting results.) Ms. Thurman said[a] such small amounts could be detected because the sample was concentrated by evaporation before analysis. Another experimenter[b] reported information from a recent discussion with Maureen K. Hamilton, Laboratory Director, Environmental Sciences, the Hanford Environmental Health Foundation. Ms. Hamilton said that the 1979 analysis was made just after a new water analysis standard was issued that required analysis for gadolinium. At that time, the standard required analysis of the exact amount of gadolinium present. (Later, the standard was revised to require only a determination that the amount of gadolinium was less than 40 ppm.) Ms. Hamilton stated that the analysis was made using emission and/or absorption spectroscopy.

A letter dated August 4, 1980, reporting the analyses of samples from the later experiments in Reference 5[c] did not report a value for gadolinium.

Possible sources of the gadolinium are paint on the tank inner wall,[d] breach of cladding on gadolinium safety rods used in experiments that were alternated with these experiments,[e] and gadolinium solution that was present in the same laboratory at that time. Although all water was replaced as experiments were alternated and precautions were taken to contain gadolinium solutions, the presence of gadolinium impurity is not impossible.[f]

Although calculational results of this set of experiments are significantly low, as discussed in Section 4, evidence indicates that gadolinium impurity at the reported concentration was indeed present. Until and unless other evidence reveals otherwise, these experiments are useful as benchmark experiments, especially for low-enriched fuel rods moderated by water containing low concentrations of gadolinium.

---

[a] Private communication, Pam Thurman, April 1994.

[b] Private communication, Michael Durst, October 1994.

[c] Private communication, Sid Bierman, September 1993.

[d] Private communication, B. M. Durst, September 1994.

[e] B. M. Durst and James Mincey, private communication, September 1994.

[f] Private communication, B. M. Durst, February 1995. Although Mr. Durst believes that results of the water sample analyses cannot be discounted, he believes that it is unlikely that such a large amount of Gd could have been present in the tank. (The 10.4 g/m^3 represents about 60 grams of gadolinium in the tank.)

(The natural abundance of gadolinium in the earth's crust is 6.1 ppm.[a] Several gadolinium compounds are soluble in room-temperature water.[b])

2.4 Temperature Data

Water temperatures were recorded in logbooks for approximately ten percent of the experiments. Measured temperatures ranged from 18°C to 26°C. ONEDANT calculations with 27-group cross sections, for an infinite slab of fuel pins reflected on both sides by 15 cm of water, gave a change in k_{eff} of 0.04% between these two extremes of temperature. (The gadolinium impurity was not included.) Therefore, an estimate of the uncertainty in k_{eff} due to the effect of temperature is half of this amount, namely 0.02%.

2.5 Cluster Separations

The measurement uncertainties in cluster separation (See Table 2.) vary from 0.02 cm to 0.08 cm. To calculate the effect on k_{eff} of this uncertainty, cluster separations were reduced for several cases. Average results for three groups are summarized in Table 7.

[a] N. N. Greenwood and A. Earnshaw, *Chemistry of the Elements*, Pergamon Press, New York, p. 1426, 1984.

[b] In particular, gadolinium bromide, chloride, fluoride, iodide, dimethylphosphate, nitrate, selenate, and sulfate. (*CRC Handbook of Chemistry and Physics*, R.C. Weast, ed., CRC Press, Inc., Boca Raton, Florida, 68th edition, p. B-91, 1987.)

Table 7. Effect on k_{eff} of Uncertainty in Measured Cluster Separation.

Case Number	Δk_{eff}(%) per 0.01 cm reduction in separation[(a)]
9, 11, 12	0.005
13-19	0.006[(b)]
20-23	-0.017

(a) KENO V.a with 27-group ENDF/B-IV cross sections.
(b) Y-separation was reduced by 0.03 cm (the average y-separation uncertainty) and x-separation was reduced by 0.08 cm; the resulting Δk_{eff} was then divided by 8 to find the effect per 0.01 cm.

The uncertainties to be included in the benchmark-model k_{eff} due to uncertainty in the cluster separation measurement are listed in Table 8. Cases that are not listed were single-cluster configurations.

Table 8. Uncertainties in Benchmark-Model k_{eff} Due to Cluster Separation Measurement Uncertainty.

Case Number	Uncertainty in Separation Measurement (cm)	Δk_{eff}(%) to Include in Uncertainty of Benchmark-Model k_{eff}
9	0.08	0.04
10	0.02	0.03[(a)]
11, 12	0.08	0.04
13-19	0.08[(b)]	0.05
20	0.03	0.05
21-23	0.02	0.03

(a) This is the only two-cluster experiment in this set of experiments. A conservative estimate is to use results from 3-cluster experiments, Cases 20-23, which give 0.017 Δk_{eff}(%) per 0.01 cm.

(b) This is x-separation uncertainty. Y-separation uncertainty varies from 0.02 to 0.04. (See footnote b of preceding table.)

3.0 BENCHMARK SPECIFICATIONS

3.1 Description of Model

The calculational models consist of square-pitched, aluminum-clad cylindrical fuel pins in water arranged in rectangular clusters. Descriptions of the critical configurations, including cluster dimensions, separations, and fuel rod pitch, are given in Table 2 and are shown in Figures 5-8.

Fractional rows for the single clusters of Cases 1 through 8 are modeled by a partial row along one side of the array that begins at the corner of the array. For Cases 9 through 12, with two or four clusters, the rods of the two partial rows for each case are added from the upper, outermost corners. (See Figure 10.) Any fraction of a rod is dropped.

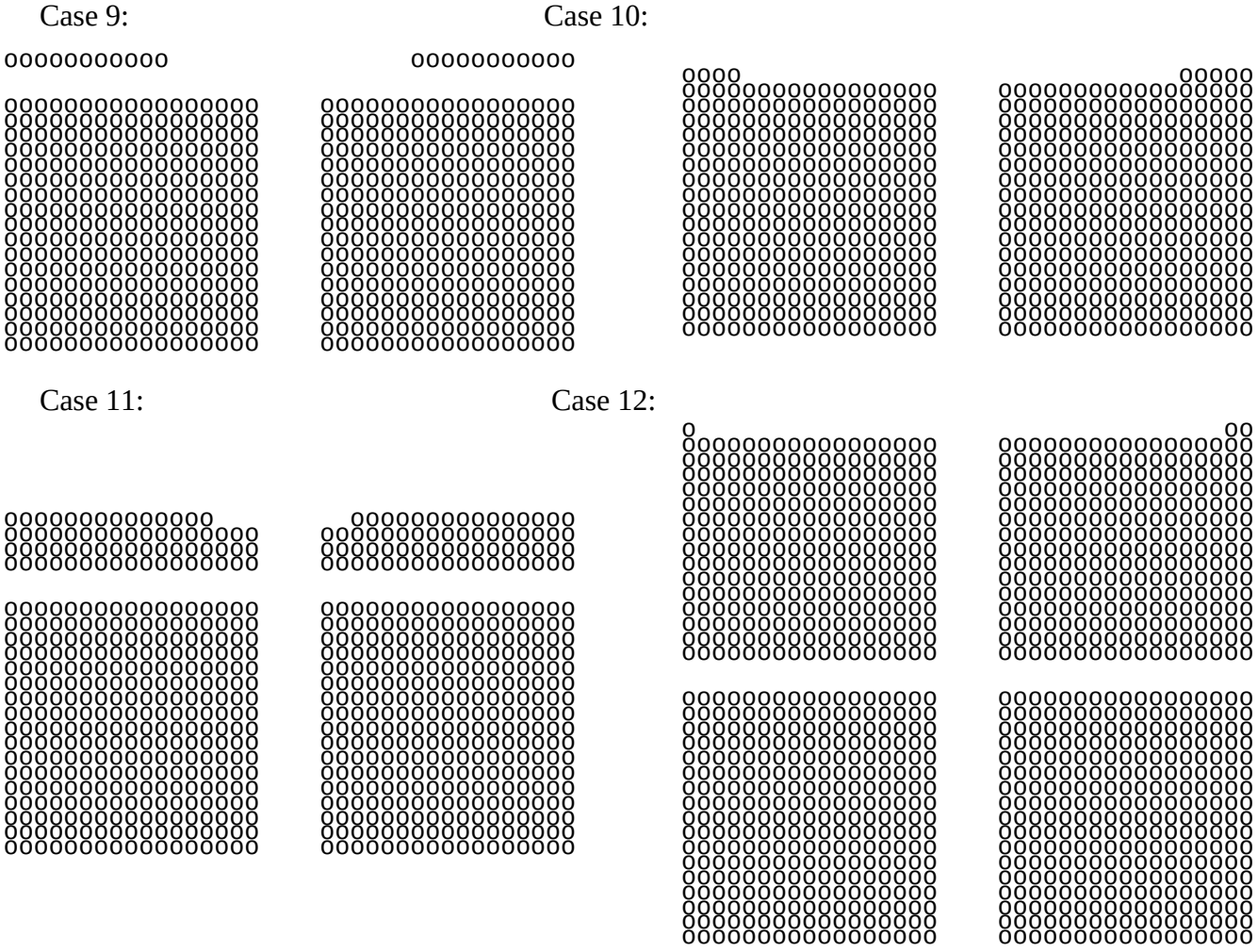

Figure 10. Partial Row Placement for Cases 9-12.

Sensitivity Studies. Two sensitivity studies were performed. One study provided a conservative estimate of the effects of discarding the fraction of a rod. A ONEDANT cylindrical homogeneous model of an array of pins was used, with the extra rod adding to the diameter of the cylinder and, therefore, effectively spread out around the outer radius of the cylinder. The effect was less than 0.03% Δk_{eff}. This is a small effect; therefore, dropping the fraction of a rod from the benchmark model is justified. However, half of this difference, namely 0.015%, which represent the effect of an average fractional rod, may be added to the uncertainty in the benchmark model k_{eff}.

Another study, using KENO V.a with 27-group cross sections, compared rods of the partial row placed at the end of the row, as in the benchmark model, to rods of the partial row placed at the center of the side. This comparison was made for five typical cases. Differences varied from 0.02% to 0.10%, with an average difference of 0.06%. Half of this may also be added to the uncertainty in the benchmark-model k_{eff}.

3.2 Dimensions

Fuel rod dimensions, as modelled, are shown in Figure 11. The entire rod has a diameter of 1.27 cm and is 97.79 cm long. The UO_2 fuel region has a diameter of 1.1176 cm and is 91.44 cm long. The clad is 0.0762 cm thick and 93.19 cm long. The clad surrounds the fuel, the lower end plug, and 0.48 cm of the top end plug. There is no gap between the clad and fuel or end plugs. The top end plug is 5.08 cm long. The lower end plug is 1.27 cm long.

The twenty-five aluminum clad voids and water-filled aluminum tubes were modeled with aluminum tubes of the same length and diameters as the fuel tubes. The aluminum clad voids had half-inch-long 6061 aluminum plugs in both ends of the tubes.

The bottom reflector is a single 2.54-cm-thick acrylic plate, which extends horizontally to the outermost cell-boundary edges of the clusters, followed by 15.3 cm of water. The four side reflectors are 30-cm-thick water. The top reflector is 9.92 cm of water.

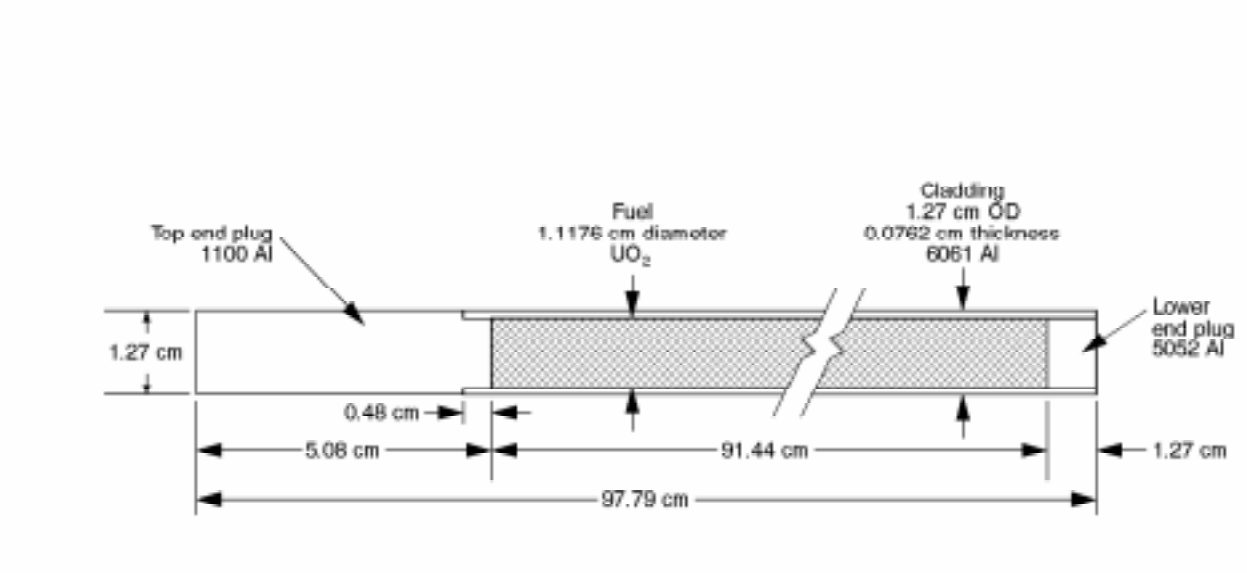

Figure 11. Fuel Rod Model.

3.3 Material Data

3.3.1 Fuel Rods - The fuel region consists of 825 g of UO_2. The mass of ^{235}U in each rod is 17.08 g. The isotopic composition of the uranium is 0.0137 wt.% ^{234}U, 2.35 wt.% ^{235}U, 0.0171 wt.% ^{236}U, and 97.6192 wt.% ^{238}U.[a]

Fuel rods have 6061 aluminum clad, with a 5052 aluminum lower end plug and a 1100 aluminum top end plug, as shown in Figure 11. Aluminum clad and end-plug components are nominal, mid-range, half-maximum, or minimum values, totalling 100 wt.%, as given in Table 4. Atom densities are given in Table 9.

[a] This is slightly less than the wt.% for ^{238}U of 97.62 quoted in Section 1, in order that all weight percents add to 100. It is inferred from a footnote to Table I, Reference 13, Vol. 2, p. 3, that the wt.% of ^{238}U is the balance. Therefore, the ^{238}U wt.% of the benchmark model is determined by balance.

Table 9. Fuel Rod Atom Densities.

Material	Isotope	Wt.%	Atom Density (barn-cm)$^{-1}$
U(2.35)O_2 fuel	^{234}U		2.8563×10^{-6}
	^{235}U		4.8785×10^{-4}
	^{236}U	-	3.5348×10^{-6}
	^{238}U		2.0009×10^{-2}
	O		4.1202×10^{-2}
1100 Aluminum	Al	99.0	5.9660×10^{-2}
(top end plug; 2.70 g/cm^3)	Cu	.12	3.0705×10^{-5}
	Mn	.025	7.3991×10^{-6}
	Zn	.05	1.2433×10^{-5}
	Si	.4025	2.3302×10^{-4}
	Fe	.4025	1.1719×10^{-4}
5052 Aluminum	Al	96.65	5.8028×10^{-2}
(lower end plug; 2.69 g/cm^3)	Cr	.25	7.7888×10^{-5}
	Cu	.05	1.2746×10^{-5}
	Mg	2.5	1.6663×10^{-3}
	Mn	.05	1.4743×10^{-5}
	Zn	.05	1.2387×10^{-5}
	Si	.225	1.2978×10^{-4}
	Fe	.225	6.5265×10^{-5}
6061 Aluminum	Al	97.325	5.8433×10^{-2}
(clad; 2.69 g/cm^3)	Cr	.2	6.2310×10^{-5}
	Cu	.25	6.3731×10^{-5}
	Mg	1.0	6.6651×10^{-4}
	Mn	.075	2.2115×10^{-5}
	Ti	.075	2.5375×10^{-5}
	Zn	.125	3.0967×10^{-5}
	Si	.6	3.4607×10^{-4}
	Fe	.35	1.0152×10^{-4}

Sensitivity Studies. In order to test the sensitivity of the critical configurations to the small amounts of alloying substances in the aluminum, a near-critical, cylindrical, water-reflected lattice of rods at a pitch of 2.032 cm was used. The thickness of the clad was increased so that the clad volume was equal to the volume of the actual clad plus the two end plugs. Therefore, this calculation is a conservative estimate of the effects of varying the clad composition.

Four cases were calculated with ONEDANT. Clad for the four cases were each of the three alloys plus pure aluminum. Results are given in Table 10. The greatest change is 0.16%, when pure aluminum clad is used. Therefore, to more accurately represent the fuel rods for this benchmark, nominal amounts of all constituents are included in the specified aluminum alloys.

Table 10. Results of ONEDANT Calculations of k_{eff} for Cylindrical Arrangements of $U(2.35)O_2$ Fuel Rods with Different Aluminum Claddings.[(a)]

Clad Material (thickness increased from 0.07620 cm to 0.09788 cm)	Δk_{eff} (%, ONEDANT) 1.684 cm pitch
6061 aluminum[(b)]	-
1100 aluminum[(b)]	0.01
5052 aluminum[(b)]	0.10
aluminum[(c)]	0.16

(a) 27-group homogenized fuel-rod mixture cross sections created by CSASIX.
(b) Alloys contain minimum amounts of aluminum and maximum amounts of other components (See Tables 4 and 9.).
(c) Density is nominal ^{27}Al density of 6061 aluminum alloy (97.325 wt.% of 2.69 g/cm^3).

3.3.2 Moderator-Reflector - Fuel rods rest on an acrylic support plate, with a density of 1.185 g/cm^3 and a composition of 8 wt.% hydrogen, 60 wt.% carbon, and 32 wt.% oxygen. The moderator-reflector is water at a temperature of 22°C. Atom densities are given in Table 11. Note that Cases 22 and 23 do not include the gadolinium impurity.

Table 11. Moderator-Reflector Atom Densities.

Material	Isotope	Atom Density $(barn\text{-}cm)^{-1}$
Water[(a)]	H O (Gd)[(b)]	6.6706×10^{-2} 3.3353×10^{-2} (3.9828×10^{-8})
Acrylic	H C O	5.6642×10^{-2} 3.5648×10^{-2} 1.4273×10^{-2}

(a) This is 0.997766 g/cm^3, interpolated from densities at 20 and 25°C (CRC Handbook of Chemistry and Physics, 68th edition, p F-10.).

(b) This is 10.4 g/m^3 of gadolinium, which is the analyzed average concentration of three water sample analyses for the experiments of Reference 4. The individual sample values were 12.0, 6.3, and 13.0 mg/l of gadolinium, resulting in a standard deviation of 3.6 g/m^3. Therefore, Cases 1-21, which are configurations from Reference 4, as indicated in Table 2, include gadolinium. Cases 22 and 23 from References 5 and 6 do not include gadolinium.

Sensitivity Studies. *Water Impurities*. The effects on k_{eff} of impurities in the water moderator-reflector for a near-critical cylindrical cluster of $U(2.35)O_2$ fuel pins, as calculated by ONEDANT, are given in Appendix C. All impurities except boron and gadolinium affect the calculated value of k_{eff} by less than 0.005%. No boron impurity was recorded for experiments included in this evaluation. However, the reported gadolinium concentration of 10.4 g/m^3 in Reference 4 caused a significant reduction (~0.8%) in k_{eff}. Results of a sensitivity study with ONEDANT slab and cylindrical geometries are given in Table 12 and shown in Figure 12.

Table 12. Effects on k_{eff} for $U(2.35)O_2$ Fuel Pins of Gadolinium Impurity in the Water Moderator-Reflector.

Quantity	Gadolinium Concentration (g/m^3)	Gadolinium Atom Density (atoms/barn-cm)	Δk_{eff}(%) ONEDANT slab geometry	Δk_{eff}(%) ONEDANT cylindrical geometry
no impurity	0	0	-	-
standard deviation of three sample measurements of impurity	3.6	1.3787×10^{-8}	-0.22	-0.29
average measured concentration minus the standard deviation	6.8	2.6042×10^{-8}	-0.41	-0.54
average measured concentration	10.4	3.9828×10^{-8}	-0.61	-0.79
average measured concentration plus the standard deviation	14.0	5.3615×10^{-8}	-0.78	-1.03

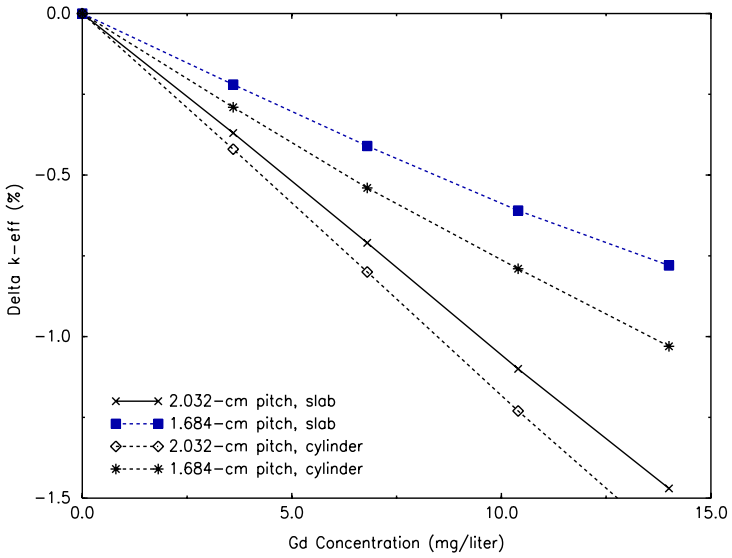

Figure 12. Change in k_{eff} with Gd Concentration (ONEDANT).

Note that the magnitude of the effect of gadolinium is greater for the near-critical cylinders than for infinite slabs. Because a reflected cylindrical cluster better represents the critical configurations evaluated here, the cylindrical results are used to determine an uncertainty in k_{eff} due to the gadolinium impurity.

The effect of the 3.6 g/m^3 uncertainty in gadolinium concentration on k_{eff} for a cylindrical cluster is 0.29% for 1.684-cm pitch rods. This may be added to the uncertainty in k_{eff} for the benchmark model.[a]

Table 13 gives Monte Carlo calculated results for nine arbitrarily chosen evaluated configurations with and without 10.4 g/m^3 gadolinium in the water of the reflector and moderator. As expected, gadolinium reduces k_{eff} by approximately 1% for fuel rods at 1.684 cm pitch.

(Note that if the gadolinium cross sections are in error, then the magnitudes of the calculated uncertainties in the benchmark-model k_{eff} due to gadolinium will also be in error.)

[a] For References 5 and 6, which do not report a gadolinium impurity, it is not certain whether gadolinium was not measured or was measured and found to be too small to report. Therefore, for the two cases (Cases 22 and 23) from these references, the uncertainty from Gd impurity may be taken to be the entire average measured Gd impurity from Reference 4. The effect on k_{eff} of the 10.4 g/m^3 of gadolinium impurity is 0.79%. This uncertainty can be included in the uncertainty in the benchmark-model k_{eff} for those two cases.

Table 13. Calculated Results[(a)] for Cases 13-22, $U(2.35)O_2$ Fuel Rods, 1.684-cm Pitch in Water, with and without Gadolinium Impurity in Water.

Code (Cross Section Set)→ / Case Number ↓	KENO (Hansen-Roach)[(b)]	KENO (Hansen-Roach)[(b)] w/o Gd in water	KENO (27-Group ENDF/ B-IV)	KENO (27-Group ENDF/ B-IV) w/o Gd in water	MCNP (continuous ENDF/ B-V)	MCNP (continuous ENDF/B-V) w/o Gd in water
13	0.9698	0.9820	0.9805	0.9873	0.9830	0.9942
14	0.9668	0.9823	0.9786	0.9905	0.9854	0.9950
15	0.9708	0.9802	0.9803	0.9889	0.9820	0.9919
16	0.9669	0.9788	0.9783	0.9887	0.9843	0.9960
17	0.9655	0.9785	0.9792	0.9874	0.9873	0.9924
18	0.9671	0.9793	0.9769	0.9882	0.9820	0.9917
19	0.9710	.9814	0.9747	0.9865	0.9859	0.9910
20	0.9617	0.9744	0.9772	0.9847	0.9814	0.9932
21,22	0.9729	0.9746	0.9788	0.9841	0.9799	0.9934
Average of above nine cases	0.9681	0.9791	0.9783	0.9874	0.9835	0.9932
Average change in k_{eff} when Gd is removed	-	+1.1%	-	+0.93%	-	0.99%

(a) Standard deviations of calculations of k_{eff} ranged from 0.0012 to 0.0019.
(b) Cross sections were the original Hansen-Roach 16-group set, except for the following: ^{234}U and ^{236}U (Mihalczo Mod of H-R U-238); Cr (AEROJET); Cu, Mg, Mn, Si (XSDRN); Ti, Zn, and Gd (GAM-2).

Bottom Reflector. The model of the bottom reflector is 2.54 cm of acrylic followed by 15.3 cm of water. The effects on k_{eff} of the one-inch-thick acrylic support plate directly beneath the fuel rods and the carbon-steel tank 17.84 cm below the fuel rods were calculated using ONEDANT. Results are shown in Table 14. The conclusions are that replacing the carbon steel tank with water has no effect, and replacing the acrylic support plate with water has a small effect (0.06%). Therefore, the support plate is retained in the benchmark model.

Because of the negligible effect of materials beyond the water reflector region (See Section 2.2.), concrete floors and walls are not included in the benchmark model.

Table 14. Calculated Effect[(a)] of Bottom Reflector Materials on k_{eff}.

Reflector			Δk_{eff} (%)
Inner 2.54 cm	Middle 15.3 cm	Outer 0.952 cm	
acrylic	water	carbon steel	-
acrylic	water	water	-0.00
water	water	water	-0.06

(a) ONEDANT slab model with CSAS 27-group cross sections and homogeneous fuel region mixture created by XSDRNPM. Reflector materials are on both sides of an infinite slab of the homogenized fuel-pin mixture.

Lattice Plates. The two polypropylene lattice plates are omitted from the benchmark model. The effects of the lattice plates are determined by another reflector sensitivity study. ONEDANT with CSAS 27-group cross sections and two homogeneous fuel region mixtures, created by XSDRNPM, is used. One fuel pin mixture has water moderator and the other has polypropylene moderator. The uppermost lattice plate is located at approximately 30 cm above the middle of the fuel pins, and the lower lattice plate rests on the acrylic support plate, just below the fuel region. The effect of the bottom lattice plate is calculated to be -0.010% Δk_{eff}, and the effect of the top lattice plate is calculated to be +0.015% Δk_{eff}. Therefore, the combined effect is approximately 0.005% Δk_{eff}. Since lattice plates are omitted from the benchmark model, this small positive contribution to k_{eff} may be subtracted from the benchmark-model k_{eff}. However, the effect is so small (less than 0.01%), the effect on k_{eff} of the lattice plates may be neglected.

3.4 Temperature Data

Temperature data for the individual experiments were not published.

Logbook records give temperature data for approximately every tenth experiment. Recorded values vary between 18°C and 26°C, with most values between 20°C and 25°C. An approximate temperature of 22°C (295 K) was used in the models.

A sensitivity study of temperature variation (See Section 2.4) demonstrated that the effects on k_{eff} of temperature were small (less than 0.005% per degree C). The effect is included in the uncertainty of the benchmark-model k_{eff}. Therefore, any reasonable approximation to room temperature may be used in the model.

3.5 Experimental and Benchmark-Model k_{eff}

The reported configurations were extrapolations to critical configurations. Therefore the experimental k_{eff} was 1.000.

Because model simplifications (no aluminum support structures; no reflector beyond 30 cm of water on the sides, 15 cm of water above, and 15.3 cm of water below; no measurement devices in the water, no notch in the top end plug; no lattice plates) were judged to have negligible effects on k_{eff}, the benchmark-model k_{eff} is 1.0000. However, some experimental uncertainties and model simplifications, described in sensitivity studies above, contribute to the estimated uncertainty in the benchmark-model k_{eff}. Those included are listed in Table 15.

Table 15. Uncertainty in Benchmark-Model k_{eff}.

Measurement Uncertainty or Model Simplification	Δk_{eff}	
Fuel rod characterization	0.0025	
Temperature	0.0002	
Cluster Separation	Case 9	0.0004
	Case 10	0.0003
	Cases 11-12	0.0004
	Cases 13-19	0.0005
	Case 20	0.0005
	Cases 21-22	0.0003
Omit fractional rod	0.00015	
Placement of partial row	0.0003	
Gadolinium impurity uncertainty (±3.6 g/m3)[(a)]	0.0029	
Total Uncertainty in k_{eff}[(b)]	0.0039	

(a) If the entire 10.4 g/m^3 Gd impurity concentration from Reference 4 is considered to be the uncertainty, as discussed in Section 3.3.2, the uncertainty in k_{eff} due to gadolinium impurity is 0.0079.

(b) Square root of sum of squares of individual Δk_{eff} values. Including the uncertainty from the entire 10.4 g/m^3 Gd impurity in the total uncertainty in k_{eff} gives 0.0083 rather than 0.0039.

Therefore, the benchmark-model k_{eff} is 1.0000 ± 0.0039.

4.0 RESULTS OF SAMPLE CALCULATIONS

Results of calculations representing the twenty-two critical configurations are presented in Tables 16 and 17. Code versions and modelling options are discussed briefly in paragraphs preceding the input listings in Appendix A.

All results are below the benchmark-model k_{eff} of 1.0000. In fact, all results of all three codes are below the range of k_{eff} that includes the estimated uncertainty. Even considering the entire reported amount of gadolinium impurity as an uncertainty, so that the uncertainty in k_{eff} is ±0.0083, all results are outside the estimated uncertainty in k_{eff}. KENO with Hansen-Roach cross sections underpredicts k_{eff} by approximately 3%[a]. KENO with 27-group ENDF/B-IV cross sections underpredicts by approximately 2%. MCNP with ENDF/B-V continuous cross sections underpredicts by 1½-2%.[b]

A possible cause of the low results for the KENO 27-group calculations is provided by the SCALE4 reference manual. Section M4.B.4, Known Cross-Section Irregularities, states the following:

> Systems containing gadolinium have not calculated well with the 27-group library. The problem stems from the characteristic of the gadolinium data in the thermal range. Gadolinium has low energy resonance data down to 10^{-5} eV. The resonances are so broad that the implementation of the Nordheim treatment in NITAWL-II fails to have a mesh point in group 27 of the 27-group structure. This has been addressed by setting the bottom energy of the resonance data to that of group 26 and carrying infinite dilution cross sections in group 27 of the master library. Use of the gadolinium in the SCALE system, especially for very dilute systems, should be done with caution.

Another possible cause is the ENDF/B-IV evaluation of ^{238}U. According to W. Rothenstein, "Thermal-Reactor Lattice Analysis Using ENDF/B-IV Data with Monte Carlo Resonance Reaction Rates," Nuclear Science and Engineering, 1976, vol. 59, pp. 337-349, the ENDF/B-IV representation of the low-lying ^{238}U resonances leads to low eigenvalues (by approximately 1%) for water-reflected low-enriched UO_2 lattices.

---

[a] Note that the gadolinium cross sections used in the KENO Hansen-Roach calculations are actually GAM-2 cross sections, rather than Hansen-Roach cross sections.

[b] A possible contribution to low MCNP results is a slight Doppler broadening at 300 K, the temperature of the cross section set, of the sharp, tall Gd resonances. This temperature is just above the temperature range of the experiments.

Note that the highest calculated value for all three codes is for Case 23, a case with no gadolinium impurity. However, even for this case, codes underpredict by 1% (MCNP and KENO 27-group) and 2% (KENO Hansen-Roach). This indicates that, besides a possible overestimation by the codes of the negative effect of gadolinium, there is some other negative influence biasing the result.[a]

Table 16. Sample Calculation (United States).

Code (Cross Sections Set)→ Case Number ↓	KENO (Hansen-Roach)[(a)]	KENO (27-Group ENDF/B-IV)	MCNP (Continuous Energy ENDF/B-V)
1	0.9651 ± .0017	0.9813 ± .0012	0.9834 ± .0017
2	0.9661 ± .0017	0.9831 ± .0012	0.9859 ± .0017
3	0.9696 ± .0018	0.9796 ± .0012	0.9841 ± .0018
4	0.9698 ± .0016	0.9803 ± .0012	0.9862 ± .0018
5	0.9670 ± .0017	0.9786 ± .0013	0.9872 ± .0016
6	0.9673 ± .0017	0.9807 ± .0013	0.9801 ± .0018
7	0.9726 ± .0018	0.9828 ± .0018	0.9859 ± .0017
8	0.9729 ± .0019	0.9825 ± .0018	0.9879 ± .0016
9	0.9673 ± .0017	0.9749 ± .0016	0.9827 ± .0018
10	0.9650 ± .0018	0.9731 ± .0018	0.9808 ± .0016
11	0.9707 ± .0016	0.9803 ± .0015	0.9838 ± .0016
12	0.9707 ± .0016	0.9759 ± .0017	0.9790 ± .0016

(a) Cross sections were the original Hansen-Roach 16-group set, except for the following: ^{234}U and ^{236}U (Mihalczo Mod of H-R U-238); Cr (AEROJET); Cu, Mg, Mn, Si (XSDRN); Ti, Zn, and Gd (GAM-2).

[a] Calculations by Westinghouse Electric Corporation, Commercial Nuclear Fuel Division, of $U(4.31)O_2$ fuel rods in water containing 10.4 g/m^3 Gd, using a proprietary 227-group ENDF/B-V library collapsed to 27 groups produced results that are generally in good agreement with the benchmark-model k_{eff}. See Appendix E of LEU-COMP-THERM-004.

Table 17. Sample Calculation Results (United States).

Code (Cross Sections Set)→ Case Number ↓	KENO (Hansen-Roach)[(a)]	KENO (27-Group ENDF/B-IV)	MCNP (Continuous Energy ENDF/B-V)
13	0.9698 ± .0016	0.9805 ± .0018	0.9849 ± .0017
14	0.9668 ± .0017	0.9786 ± .0017	0.9830 ± .0019
15	0.9708 ± .0018	0.9803 ± .0016	0.9856 ± .0018
16	0.9669 ± .0017	0.9783 ± .0016	0.9845 ± .0017
17	0.9655 ± .0017	0.9792 ± .0017	0.9802 ± .0018
18	0.9671 ± .0017	0.9769 ± .0017	0.9829 ± .0016
19	0.9710 ± .0015	0.9747 ± .0016	0.9838 ± .0018
20	0.9617 ± .0018	0.9772 ± .0018	0.9853 ± .0018
21	0.9631 ± .0017	0.9800 ± .0017	0.9835 ± .0017
22	0.9761 ± .0018	0.9832 ± .0016	0.9895 ± .0017
23	0.9818 ± .0017	0.9892 ± .0017	0.9907 ± .0017

(a) Cross sections were the original Hansen-Roach 16-group set, except for the following: ^{234}U and ^{236}U (Mihalczo Mod of H-R U-238); Cr (AEROJET); Cu, Mg, Mn, Si (XSDRN); Ti, Zn, and Gd (GAM-2).

5.0 REFERENCES

1. S. R. Bierman, E. D. Clayton, and B. M. Durst, "Critical Separation Between Subcritical Clusters of 2.35 Wt% ^{235}U Enriched UO_2 Rods in Water with Fixed Neutron Poisons," PNL-2438, Battelle Pacific Northwest Laboratories, Richland, Washington, October 1977.

2. S. R. Bierman, B. M. Durst, and E. D. Clayton, "Critical Separation Between Subcritical Clusters of 4.29 Wt% ^{235}U Enriched UO_2 Rods in Water with Fixed Neutron Poisons," NUREG/CR-0073, Battelle Pacific Northwest Laboratories, Richland, Washington, May 1978.

3. S. R. Bierman, B. M. Durst, and E. D. Clayton, "Criticality Experiments with Subcritical Clusters of 2.35 Wt% and 4.29 Wt% ^{235}U Enriched UO_2 Rods in Water with Uranium or Lead Reflecting Walls, Near Optimum Water-to-Fuel Volume Ratio," NUREG/CR-0796, Vol. 1, PNL-2827, Battelle Pacific Northwest Laboratories, Richland, Washington, April 1979.

4. S. R. Bierman, and E. D. Clayton, "Criticality Experiments with Subcritical Clusters of 2.35 Wt% and 4.31 Wt% ^{235}U Enriched UO_2 Rods in Water at a Water-to-Fuel Volume Ratio of 1.6," NUREG/CR-1547, PNL-3314, Battelle Pacific Northwest Laboratories, Richland, Washington, July 1980.

5. S. R. Bierman, and E. D. Clayton, "Criticality Experiments with Subcritical Clusters of 2.35 Wt% and 4.31 Wt% ^{235}U Enriched UO_2 Rods in Water with Steel Reflecting Walls," NUREG/CR-1784, PNL-3602, Battelle Pacific Northwest Laboratories, Richland, Washington, April 1981.

6. S. R. Bierman, B. M. Durst, and E. D. Clayton, "Criticality Experiments with Subcritical Clusters of 2.35 Wt% and 4.31 Wt% ^{235}U Enriched UO_2 Rods in Water with Uranium or Lead Reflecting Walls, Undermoderated Water-to-Fuel Volume Ratio of 1.6," NUREG/CR-0796, PNL-3926, Vol. 2, Battelle Pacific Northwest Laboratories, Richland, Washington, December 1981.

7. B. M. Durst, S. R. Bierman, and E. D. Clayton, "Critical Experiments with 4.31 Wt% ^{235}U Enriched UO_2 Rods in Highly Borated Water Lattices," NUREG/CR-2709, PNL-4267, Battelle Pacific Northwest Laboratories, Richland, Washington, August 1982.

8. S. R. Bierman, E. S. Murphy, E. D. Clayton, and R. T. Keay, "Criticality Experiments with Low Enriched UO_2 Fuel Rods in Water Containing Dissolved Gadolinium," PNL-4976, Battelle Pacific Northwest Laboratories, Richland, Washington, February 1984.

9. S. R. Bierman, "Criticality Experiments to Provide Benchmark Data on Neutron Flux Traps," PNL-6205, UC-714, Battelle Pacific Northwest Laboratories, Richland, Washington, June 1988.

10. S. R. Bierman, "Criticality Experiments with Neutron Flux Traps Containing Voids," PNL-7167, TTC-0969, UC-722, Battelle Pacific Northwest Laboratories, Richland, Washington, April 1990.

11. B. M. Durst, S. R. Bierman, E. D. Clayton, J.F. Mincey, and R.T. Primm III, "Summary of Experimental Data for Critical Arrays of Water Moderated Fast Test Reactor Fuel," PNL-3313, ORNL/Sub-81/97731/1, Battelle Pacific Northwest Laboratories, Richland, Washington, May 1981.

12. S. R. Bierman, B. M. Durst, and E. D. Clayton, "Critical Separation between Subcritical Clusters of Low Enriched UO_2 Rods in Water with Fixed Neutron Poisons," Nuc. Technol., **42**, pp. 237-249, March 1979.

13. R. I. Smith and G. J. Konzek, principal investigators, "Clean Critical Experiment Benchmarks for Plutonium Recycle in LWR's, NP-196," Volumes 1 and 2, Battelle Pacific Northwest Laboratories, Richland, Washington, April 1976, and September 1978.

14. S. R. Bierman and E. D. Clayton, "Criticality Experiments with Subcritical Clusters of 2.35 and 4.31 wt% ^{235}U-Enriched UO_2 Rods in Water with Steel Reflecting Walls," Nuc. Technol., **54**, August 1981.

15. S. R. Bierman, B. M. Durst, and E. D. Clayton, "Criticality Experiments with Subcritical Clusters of Low Enriched UO_2 Rods in Water with Uranium or Lead Reflecting Walls," Nuc. Technol., **47**, January 1980.

APPENDIX A: TYPICAL INPUT LISTINGS

A.1 KENO Input Listings

The version of KENO V.a used was SCALE 4.0 (creation date: 08/09/91, for standalone KENO V.a with Hansen-Roach Cross Sections, provided by the Radiation Shielding Information Center; creation date: 07/20/92, for KENO V.a with CSAS 27-Group ENDF/B-IV Cross Sections).

KENO V.a input files were created with arrays of fuel rod units. Cuboids of water were used to complete partial rows. Larger cuboids of water provided the separation between clusters of rods.

KENO V.a was run using 110 active generations of 1500 neutrons each, after skipping 50 generations, for a total of 165,000 averaged neutron histories. For 27-group calculations for Cases 1-6, which were also used in sensitivity studies, more neutrons (185,000) were used.

The resonance correction used to determine the Hansen-Roach cross section IDs for ^{235}U and ^{238}U was calculated using the formula

$$\sigma_{pj} = \sum_{i}^{n} \frac{\sigma_{si} N_i}{N_j} + \frac{1 - C}{2 r_f N_j}$$

σ_{pj} is the resonance correction for the j^{th} fissile nuclide. N_i is the atom density of the i^{th} nuclide in the fuel mixture, n is the number of different nuclides in the fuel mixture, and σ_{si} is the scattering cross section in the resonance region for the i^{th} component of the mixture. Values used for σ_{si} were 12 for uranium and 3.7 for oxygen. Linear interpolation was used to apportion atom densities between the two uranium cross section sets whose σ_p values were closest to the calculated σ_p.

The last term is the Wigner-Rational correction. C is the Dancoff correction factor and r_f is the radius of the cylindrical fuel region of the fuel rod. (The value of C, the Dancoff correction factor, calculated by CSAS, was 0.2011 for 1.684 cm pitch.)

KENO-V.a Input Listing for Case 3 of Table 16 (16-Energy-
Group Hansen-Roach Cross Sections).

```
KG11  23X22.78 (23X22 + 17 RODS) AT 1.684 CM PITCH
READ PARA TME=200 GEN=160 NPG=1500 NSK=50 NUB=YES
LIB=41 XS1=YES RUN=YES LNG=60000    END PARA
READ MIXT  SCT=3 MIX=1
' U(2.35)02 for 1.684 cm pitch
92400 2.8563-6  92509 4.1902-4  92510 6.8826-5
92600 3.5348-6  92857 4.3594-3  92858 1.5650-2
8100 4.1202-2
MIX=2
' water
1102 6.6706-2   8100 3.3353-2  64100 3.9828-8
MIX=3
' 6061 Al (clad)
13100 5.8433-2  24100 6.2310-5  29100 6.3731-5
12100 6.6651-4  25100 2.2115-5  22100 2.5375-5
30100 3.0967-5  14100 3.4607-4  26100 1.0152-4
MIX=4
'  1100 Al (top end plug)
13100 5.9660-2  29100 3.0705-5  25100 7.3991-6
30100 1.2433-5  14100 2.3302-4  26100 1.1719-4
MIX=5
' 5052 Al (lower end plug)
13100 5.8028-2  24100 7.7888-5  29100 1.2746-5
12100 1.6663-3  25100 1.4743-5  30100 1.2387-5
14100 1.2978-4  26100 6.5265-5
MIX=6
' acrylic
1102 5.6642-2  6100 3.5648-2  8100 1.4273-2
END MIXT
READ GEOM
UNIT 1
 COM=* FUEL PIN *
 CYLINDER  1 1  0.5588 91.44 0.0
 CYLINDER  4 1  0.5588 91.92 0.0
 CYLINDER  5 1  0.5588 91.92 -1.27
 CYLINDER  3 1  0.635  91.92 -1.27
 CYLINDER  4 1  0.635  96.52 -1.27
 CUBOID  2 1  4P.842 96.52 -1.27
UNIT 2
 COM=* WATER FUEL PIN *
 CUBOID  2 1  4P.842 96.52 -1.27
UNIT 3
 COM=* 23X22 CLUSTER *
 ARRAY 1 3R0
UNIT 4
 COM=* 17 RODS AT END OF ROW *
 ARRAY 2 3R0
GLOBAL
UNIT 5
 COM=* 23X22 CLUSTER WITH 17 RODS ADDED *
 ARRAY 3 3R0
 REPLICATE 6 1  5R0.0 2.54  1
 REPLICATE 2 1  4R30.0 9.92 15.3  1
END GEOM
READ ARRAY  ARA=1 NUX=23 NUY=22  FILL F1 END FILL
         ARA=2 NUX=23 NUY=1  FILL  17R1 6R2  END FILL
         ARA=3 NUY=2 FILL 3 4 END FILL
END ARRAY
END DATA
END
```

KENO-V.a Input Listing for Case 10 of Table 16 (16-Energy-Group Hansen-Roach Cross Sections).

```
KG18  ONE 17X17 +4 CLUSTER, ONE 17X17 +5 CLUSTER, 1.68 CM
SEPARATION
READ PARA TME=200 GEN=160 NPG=1500 NSK=50 NUB=YES
LIB=41 XS1=YES RUN=YES LNG=60000    END PARA
READ MIXT  SCT=3
MIX=1
' U(2.35)02 for 1.684 cm pitch
92400 2.8563-6  92509 4.1902-4  92510 6.8826-5
92600 3.5348-6  92857 4.3594-3  92858 1.5650-2
8100 4.1202-2
MIX=2
' water
1102 6.6706-2   8100 3.3353-2  64100 3.9828-8
MIX=3
' 6061 Al (clad)
13100 5.8433-2  24100 6.2310-5  29100 6.3731-5
12100 6.6651-4  25100 2.2115-5  22100 2.5375-5
30100 3.0967-5  14100 3.4607-4  26100 1.0152-4
MIX=4
'  1100 Al (top end plug)
13100 5.9660-2  29100 3.0705-5  25100 7.3991-6
30100 1.2433-5  14100 2.3302-4  26100 1.1719-4
MIX=5
' 5052 Al (lower end plug)
13100 5.8028-2  24100 7.7888-5  29100 1.2746-5
12100 1.6663-3  25100 1.4743-5  30100 1.2387-5
14100 1.2978-4  26100 6.5265-5
MIX=6
' acrylic
1102 5.6642-2  6100 3.5648-2  8100 1.4273-2
END MIXT
READ GEOM
UNIT 1
 COM=* FUEL PIN *
 CYLINDER  1 1  0.5588 91.44 0.0
 CYLINDER  4 1  0.5588 91.92 0.0
 CYLINDER  5 1  0.5588 91.92 -1.27
 CYLINDER  3 1  0.635  91.92 -1.27
 CYLINDER  4 1  0.635  96.52 -1.27
 CUBOID  2 1  4P.842 96.52 -1.27
UNIT 2
 COM=* WATER CUBOID *
 CUBOID  2 1  4P.842 96.52 -1.27
UNIT 3
 COM=* 17X17 +4 ARRAY OF FUEL PINS *
 ARRAY 1 3R0
UNIT 4
 COM=* 17X17 +5 ARRAY OF FUEL PINS *
 ARRAY 2 3R0
UNIT 5
 COM=* WATER BETWEEN CLUSTERS, 1.68 CM WIDE *
 CUBOID  2 1  1.68 0.0 30.312 0.0 96.52 -1.27
GLOBAL
UNIT 6
 COM=* ARRAY OF 2 CLUSTERS, 1 IN. ACRYLIC BELOW, WATER
REFLECTOR *
 ARRAY 3 3R0
 REPLICATE 6 1  5R0.0 2.54  1
 REPLICATE 2 1  4R30.0 9.92 15.3  1
END GEOM
READ ARRAY  ARA=1 NUX=17 NUY=18  FILL 293R1 13R2 END FILL
        ARA=2 NUX=17 NUY=18  FILL 289R1 12R2 5R1 END FILL
        ARA=3 NUX=3  FILL 3 5 4  END FILL
END ARRAY
READ PLOT
  XUL=-3 YUL=1.016 ZUL=100 XLR=2.032 YLR=1.016
  ZLR=-5  UAX=1  WDN=-1 NAX=30 NDN=110 NCH=' *~ctla~' END
  XUL=-5 YUL=15 ZUL=2 XLR=15 YLR=-5
  ZLR=2   UAX=1  VDN=-1 NAX=120 NCH=' *~ctla~' END
  XUL=-5 YUL=1.016 ZUL=100 XLR=150 YLR=1.016
  ZLR=-6   UAX=1  WDN=-1 NAX=120 NCH=' *~ctla~' END
  PIC=UNIT XUL=-5 YUL=40 ZUL=2 XLR=150 YLR=-5
  ZLR=2   UAX=1  VDN=-1 NAX=120 NCH=' 12345' END
END PLOT
END DATA
END
```

KENO-V.a Input Listing for Case 11 of Table 16 (16-Energy-Group Hansen-Roach Cross Sections).

```
KG19  TWO 17X3 +14 AND +15 CLUSTERS, TWO 17X17 CLUSTERS, 4.27
CM X-SEP, Y-SEP
READ PARA TME=200 GEN=160 NPG=1500 NSK=50 NUB=YES
LIB=41 XS1=YES RUN=YES LNG=80000    END PARA
READ MIXT  SCT=3
MIX=1
' U(2.35)02 for 1.684 cm pitch
92400 2.8563-6  92509 4.1902-4  92510 6.8826-5
92600 3.5348-6  92857 4.3594-3  92858 1.5650-2
8100 4.1202-2
MIX=2
' water
1102 6.6706-2   8100 3.3353-2  64100 3.9828-8
MIX=3
' 6061 Al (clad)
13100 5.8433-2  24100 6.2310-5  29100 6.3731-5
12100 6.6651-4  25100 2.2115-5  22100 2.5375-5
30100 3.0967-5  14100 3.4607-4  26100 1.0152-4
MIX=4
'  1100 Al (top end plug)
13100 5.9660-2  29100 3.0705-5  25100 7.3991-6
30100 1.2433-5  14100 2.3302-4  26100 1.1719-4
MIX=5
' 5052 Al (lower end plug)
13100 5.8028-2  24100 7.7888-5  29100 1.2746-5
12100 1.6663-3  25100 1.4743-5  30100 1.2387-5
14100 1.2978-4  26100 6.5265-5
MIX=6
' acrylic
1102 5.6642-2  6100 3.5648-2  8100 1.4273-2
END MIXT
READ GEOM
UNIT 1
 COM=* FUEL PIN *
 CYLINDER  1 1  0.5588 91.44 0.0
 CYLINDER  4 1  0.5588 91.92 0.0
 CYLINDER  5 1  0.5588 91.92 -1.27
 CYLINDER  3 1  0.635  91.92 -1.27
 CYLINDER  4 1  0.635  96.52 -1.27
 CUBOID  2 1  4P.842 96.52 -1.27
UNIT 2
 COM=* WATER CUBOID *
 CUBOID  2 1  4P.842 96.52 -1.27
UNIT 3
 COM=* 17X17 ARRAY OF FUEL PINS *
 ARRAY 1 3R0
UNIT 4
 COM=* 17X3 +14 ROD CLUSTER *
 ARRAY 2 3R0
UNIT 5
 COM=* 17X3 +15 ROD CLUSTER *
 ARRAY 3 3R0
UNIT 6
 COM=* WATER BETWEEN CLUSTERS, 17 RODS WIDE, 4.27 CM THICK *
 CUBOID  2 1  28.628 0.0 4.27 0.0 96.52 -1.27
UNIT 7
 COM=* LEFT TWO CLUSTERS *
 ARRAY 4 3R0
UNIT 8
 COM=* RIGHT TWO CLUSTERS *
 ARRAY 5 3R0
UNIT 9
 COM=* WATER BETWEEN CLUSTERS, 4.27 CM WIDE *
 CUBOID  2 1  4.27 0.0 39.634 0.0 96.52 -1.27
GLOBAL
UNIT 10
 COM=* ARRAY OF 4 CLUSTERS, 1 IN. ACRYLIC BELOW, WATER
REFLECTOR *
 ARRAY 6 3R0
 REPLICATE 6 1  5R0.0 2.54  1
 REPLICATE 2 1  4R30.0 9.92 15.3  1
END GEOM
READ ARRAY  ARA=1 NUX=17 NUY=17  FILL F1 END FILL
        ARA=2 NUX=17 NUY=4  FILL  65R1 3R2  END FILL
        ARA=3 NUX=17 NUY=4  FILL  51R1 2R2 15R1  END FILL
        ARA=4 NUY=3  FILL 3 6 4 END FILL
        ARA=5 NUY=3  FILL 3 6 5 END FILL
        ARA=6 NUX=3  FILL 7 9 8 END FILL
END ARRAY
READ PLOT
  XUL=0 YUL=.842 ZUL=100 XLR=2.032 YLR=.842
  ZLR=-5  UAX=1  WDN=-1 NAX=20 NDN=50 NCH=' *~ctla~' END
  XUL=-5 YUL=15 ZUL=2 XLR=15 YLR=-5
  ZLR=2   UAX=1  VDN=-1 NAX=120 NDN=100 NCH=' *~ctla~' END
  XUL=-5 YUL=1.016 ZUL=100 XLR=30 YLR=1.016
  ZLR=-6 UAX=1  WDN=-1 NAX=120 NDN=60 NCH=' *~ctla~' END
  PIC=UNIT XUL=-5 YUL=40 ZUL=2 XLR=70 YLR=-5
  ZLR=2 UAX=1 VDN=-1 NAX=60 NDN=60 NCH=' 12345' END
END PLOT
END DATA
END
```

KENO-V.a Input Listing for Case 22 of Table 17 (16-Energy-Group Hansen-Roach Cross Sections).

```
K29  CENTER 25X18 CLUSTER, TWO 20X18 CLUSTERS, 6.826 CM
SEPARATION
READ PARA TME=200 GEN=160 NPG=1500 NSK=50 NUB=YES
LIB=41 XS1=YES RUN=YES LNG=60000    END PARA
READ MIXT  SCT=3
MIX=1
' U(2.35)02 for 1.684 cm pitch
92400 2.8563-6  92509 4.1902-4  92510 6.8826-5
92600 3.5348-6  92857 4.3594-3  92858 1.5650-2
8100 4.1202-2
MIX=2
' water
1102 6.6706-2   8100 3.3353-2
MIX=3
' 6061 Al (clad)
13100 5.8433-2  24100 6.2310-5  29100 6.3731-5
12100 6.6651-4  25100 2.2115-5  22100 2.5375-5
30100 3.0967-5  14100 3.4607-4  26100 1.0152-4
MIX=4
'  1100 Al (top end plug)
13100 5.9660-2  29100 3.0705-5  25100 7.3991-6
30100 1.2433-5  14100 2.3302-4  26100 1.1719-4
MIX=5
' 5052 Al (lower end plug)
13100 5.8028-2  24100 7.7888-5  29100 1.2746-5
12100 1.6663-3  25100 1.4743-5  30100 1.2387-5
14100 1.2978-4  26100 6.5265-5
MIX=6
' acrylic
1102 5.6642-2  6100 3.5648-2  8100 1.4273-2
END MIXT
READ GEOM
UNIT 1
 COM=* FUEL PIN *
 CYLINDER  1 1  0.5588 91.44 0.0
 CYLINDER  4 1  0.5588 91.92 0.0
 CYLINDER  5 1  0.5588 91.92 -1.27
 CYLINDER  3 1  0.635  91.92 -1.27
 CYLINDER  4 1  0.635  96.52 -1.27
 CUBOID  2 1  4P.842 96.52 -1.27
UNIT 2
 COM=* 25X18 ARRAY OF FUEL PINS *
 ARRAY 1 3R0
UNIT 3
 COM=* 20X18 ARRAY OF FUEL PINS *
 ARRAY 2 3R0
UNIT 4
 COM=* WATER BETWEEN CLUSTERS, 6.826 CM WIDE *
 CUBOID  2 1  6.826 0.0 30.312 0.0 96.52 -1.27
GLOBAL
UNIT 5
 COM=* ARRAY OF 3 CLUSTERS, 1 IN. ACRYLIC BELOW, WATER
REFLECTOR *
 ARRAY 3 3R0
 REPLICATE 6 1  5R0.0 2.54  1
 REPLICATE 2 1  4R30.0 9.92 15.3  1
END GEOM
READ PLOT
  XUL=-3 YUL=1.016 ZUL=100 XLR=2.032 YLR=1.016
  ZLR=-5  UAX=1  WDN=-1 NAX=30 NDN=110 NCH=' *~ctla~' END
  XUL=-5 YUL=15 ZUL=2 XLR=15 YLR=-5
  ZLR=2   UAX=1  VDN=-1 NAX=120 NCH=' *~ctla~' END
  XUL=-5 YUL=1.016 ZUL=100 XLR=150 YLR=1.016
  ZLR=-6   UAX=1  WDN=-1 NAX=120 NCH=' *~ctla~' END
  PIC=UNIT XUL=-5 YUL=40 ZUL=2 XLR=150 YLR=-5
  ZLR=2   UAX=1  VDN=-1 NAX=120 NCH=' 12345' END
END PLOT
READ ARRAY  ARA=1 NUX=25 NUY=18  FILL F1 END FILL
          ARA=2 NUX=20 NUY=18  FILL F1 END FILL
          ARA=3 NUX=5  FILL 3 4 2 4 3 END FILL
END ARRAY
END DATA
END
```

KENO-V.a Input Listing for Case 3 of Table 16 (27-Energy-Group SCALE4 Cross Sections).

```
=CSAS25
CG11  23X22.78 (23X22 + 17 RODS) AT 1.684 CM PITCH
27GROUPNDF4 LATTICECELL
' U(2.35)02
U-234  1 0  2.8563-6 295 END
U-235  1 0  4.8785-4 295 END
U-236  1 0  3.5348-6 295 END
U-238  1 0  2.0009-2 295 END
O  1 0  4.1202-2 295 END
' water with Gd
H  2 0  6.6706-2 295 END
O  2 0  3.3353-2 295 END
GD  2 0  3.9828-8 295 END
' 6061 Al (clad)
AL  3 0  5.8433-2 295 END
CR  3 0  6.2310-5 295 END
CU  3 0  6.3731-5 295 END
MG  3 0  6.6651-4 295 END
MN  3 0  2.2115-5 295 END
TI  3 0  2.5375-5 295 END
'       (Zn replaced by Cu)
CU  3 0  3.0967-5 295 END
SI  3 0  3.4607-4 295 END
FE  3 0  1.0152-4 295 END
'  1100 Al (top end plug)
AL  4 0  5.9660-2 295 END
CU  4 0  3.0705-5 295 END
MN  4 0  7.3991-6 295 END
'       (Zn replaced by Cu)
CU  4 0  1.2433-5 295 END
SI  4 0  2.3302-4 295 END
FE  4 0  1.1719-4 295 END
' 5052 Al (lower end plug)
AL  5 0  5.8028-2 295 END
CR  5 0  7.7888-5 295 END
CU  5 0  1.2746-5 295 END
MG  5 0  1.6663-3 295 END
MN  5 0  1.4743-5 295 END
'       (Zn replaced by Cu)
CU  5 0  1.2387-5 295 END
SI  5 0  1.2978-4 295 END
FE  5 0  6.5265-5 295 END
' acrylic
H   6 0  5.6642-2 295 END
C   6 0  3.5648-2 295 END
O   6 0  1.4273-2 295 END
' water with Gd
H  7 0  6.6706-2 295 END
O  7 0  3.3353-2 295 END
GD  7 0  3.9828-8 295 END
END COMP
SQUAREPITCH 1.684 1.1176 1 2 1.27 3 END
CG11  23X22.78 (23X22 + 17 RODS) AT 1.684 CM PITCH
READ PARA TME=200 GEN=200 NPG=2000 NSK=50 NUB=YES XS1=YES
RUN=YES
END PARA
READ GEOM
UNIT 1
 COM=* FUEL PIN *
 CYLINDER  1 1  0.5588 91.44 0.0
 CYLINDER  4 1  0.5588 91.92 0.0
 CYLINDER  5 1  0.5588 91.92 -1.27
 CYLINDER  3 1  0.635  91.92 -1.27
 CYLINDER  4 1  0.635  96.52 -1.27
 CUBOID  2 1  4P.842 96.52 -1.27
UNIT 2
 COM=* WATER FUEL PIN *
 CUBOID  2 1  4P.842 96.52 -1.27
UNIT 3
 COM=* 23X22 CLUSTER *
 ARRAY 1 3R0
UNIT 4
 COM=* 17 RODS AT END OF ROW *
 ARRAY 2 3R0
GLOBAL
UNIT 5
 COM=* 23X22 CLUSTER WITH 17 RODS ADDED TO END OF ROW *
 ARRAY 3 3R0
 REPLICATE 6 1  5R0.0 2.54  1
 REPLICATE 7 1  4R30.0 9.92 15.3  1
END GEOM
READ ARRAY  ARA=1 NUX=23 NUY=22  FILL F1 END FILL
        ARA=2 NUX=23 NUY=1  FILL  17R1 6R2  END FILL
        ARA=3 NUY=2 FILL 3 4 END FILL
END ARRAY
END DATA
END
```

KENO-V.a Input Listing for Case 10 of Table 16 (27-Energy-Group SCALE4 Cross Sections).

```
=CSAS25
CG18  ONE 17X17 +4 CLUSTER, ONE 17X17 +5 CLUSTER, 1.68 CM
SEPARATION
27GROUPNDF4 LATTICECELL
' U(2.35)02
U-234  1 0  2.8563-6 295 END
U-235  1 0  4.8785-4 295 END
U-236  1 0  3.5348-6 295 END
U-238  1 0  2.0009-2 295 END
O  1 0  4.1202-2 295 END
' water
H  2 0  6.6706-2 295 END
O  2 0  3.3353-2 295 END
GD  2 0  3.9828-8 295 END
' 6061 Al (clad)
AL  3 0  5.8433-2 295 END
CR  3 0  6.2310-5 295 END
CU  3 0  6.3731-5 295 END
MG  3 0  6.6651-4 295 END
MN  3 0  2.2115-5 295 END
TI  3 0  2.5375-5 295 END
'       (Zn replaced by Cu)
CU  3 0  3.0967-5 295 END
SI  3 0  3.4607-4 295 END
FE  3 0  1.0152-4 295 END
'  1100 Al (top end plug)
AL  4 0  5.9660-2 295 END
CU  4 0  3.0705-5 295 END
MN  4 0  7.3991-6 295 END
'       (Zn replaced by Cu)
CU  4 0  1.2433-5 295 END
SI  4 0  2.3302-4 295 END
FE  4 0  1.1719-4 295 END
' 5052 Al (lower end plug)
AL  5 0  5.8028-2 295 END
CR  5 0  7.7888-5 295 END
CU  5 0  1.2746-5 295 END
MG  5 0  1.6663-3 295 END
MN  5 0  1.4743-5 295 END
'       (Zn replaced by Cu)
CU  5 0  1.2387-5 295 END
SI  5 0  1.2978-4 295 END
FE  5 0  6.5265-5 295 END
' acrylic
H   6 0  5.6642-2 295 END
C   6 0  3.5648-2 295 END
O   6 0  1.4273-2 295 END
' water
H  7 0  6.6706-2 295 END
O  7 0  3.3353-2 295 END
GD  7 0  3.9828-8 295 END
END COMP
SQUAREPITCH 1.684 1.1176 1 2 1.27 3 END
CG18  ONE 17X17 +4 CLUSTER, ONE 17X17 +5 CLUSTER, 1.68 CM
SEPARATION
READ PARA TME=200 GEN=160 NPG=1500 NSK=50 NUB=YES XS1=YES
RUN=YES
END PARA
READ GEOM
UNIT 1
 COM=* FUEL PIN *
 CYLINDER  1 1  0.5588 91.44 0.0
 CYLINDER  4 1  0.5588 91.92 0.0
 CYLINDER  5 1  0.5588 91.92 -1.27
 CYLINDER  3 1  0.635  91.92 -1.27
 CYLINDER  4 1  0.635  96.52 -1.27
 CUBOID  2 1  4P.842 96.52 -1.27
UNIT 2
 COM=* WATER CUBOID *
 CUBOID  7 1  4P.842 96.52 -1.27
UNIT 3
 COM=* 17X17 +4 ARRAY OF FUEL PINS *
 ARRAY 1 3R0
UNIT 4
 COM=* 17X17 +5 ARRAY OF FUEL PINS *
 ARRAY 2 3R0
UNIT 5
 COM=* WATER BETWEEN CLUSTERS, 1.68 CM WIDE *
 CUBOID  7 1  1.68 0.0 30.312 0.0 96.52 -1.27
GLOBAL
UNIT 6
 COM=* ARRAY OF 2 CLUSTERS, 1 IN. ACRYLIC BELOW, WATER
REFLECTOR *
 ARRAY 3 3R0
 REPLICATE 6 1  5R0.0 2.54  1
 REPLICATE 7 1  4R30.0 9.92 15.3  1
END GEOM
READ ARRAY  ARA=1 NUX=17 NUY=18  FILL 293R1 13R2 END FILL
         ARA=2 NUX=17 NUY=18  FILL 289R1 12R2 5R1 END FILL
         ARA=3 NUX=3  FILL 3 5 4  END FILL
END ARRAY
READ PLOT
  XUL=-3 YUL=1.016 ZUL=100 XLR=2.032 YLR=1.016
  ZLR=-5  UAX=1  WDN=-1 NAX=30 NDN=110 NCH=' *~ctla~' END
  XUL=-5 YUL=15 ZUL=2 XLR=15 YLR=-5
  ZLR=2   UAX=1  VDN=-1 NAX=120 NCH=' *~ctla~' END
  XUL=-5 YUL=1.016 ZUL=100 XLR=150 YLR=1.016
  ZLR=-6   UAX=1  WDN=-1 NAX=120 NCH=' *~ctla~' END
  PIC=UNIT XUL=-5 YUL=40 ZUL=2 XLR=150 YLR=-5
  ZLR=2   UAX=1  VDN=-1 NAX=120 NCH=' 12345' END
END PLOT
END DATA
END
```

KENO-V.a Input Listing for Case 11 of Table 16 (27-Energy-Group SCALE4 Cross Sections).

```
=CSAS25
CG19  TWO 17X3 +14 AND +15 CLUSTERS, TWO 17X17 CLUSTERS, 4.27
CM X-SEP, Y-SEP
27GROUPNDF4 LATTICECELL
' U(2.35)02
U-234  1 0  2.8563-6 295 END
U-235  1 0  4.8785-4 295 END
U-236  1 0  3.5348-6 295 END
U-238  1 0  2.0009-2 295 END
O  1 0  4.1202-2 295 END
' water
H  2 0  6.6706-2 295 END
O  2 0  3.3353-2 295 END
GD  2 0  3.9828-8 295 END
' 6061 Al (clad)
AL  3 0  5.8433-2 295 END
CR  3 0  6.2310-5 295 END
CU  3 0  6.3731-5 295 END
MG  3 0  6.6651-4 295 END
MN  3 0  2.2115-5 295 END
TI  3 0  2.5375-5 295 END
'       (Zn replaced by Cu)
CU  3 0  3.0967-5 295 END
SI  3 0  3.4607-4 295 END
FE  3 0  1.0152-4 295 END
'  1100 Al (top end plug)
AL  4 0  5.9660-2 295 END
CU  4 0  3.0705-5 295 END
MN  4 0  7.3991-6 295 END
'       (Zn replaced by Cu)
CU  4 0  1.2433-5 295 END
SI  4 0  2.3302-4 295 END
FE  4 0  1.1719-4 295 END
' 5052 Al (lower end plug)
AL  5 0  5.8028-2 295 END
CR  5 0  7.7888-5 295 END
CU  5 0  1.2746-5 295 END
MG  5 0  1.6663-3 295 END
MN  5 0  1.4743-5 295 END
'       (Zn replaced by Cu)
CU  5 0  1.2387-5 295 END
SI  5 0  1.2978-4 295 END
FE  5 0  6.5265-5 295 END
' acrylic
H   6 0  5.6642-2 295 END
C   6 0  3.5648-2 295 END
O   6 0  1.4273-2 295 END
' water
H  7 0  6.6706-2 295 END
O  7 0  3.3353-2 295 END
GD  7 0  3.9828-8 295 END
END COMP
SQUAREPITCH 1.684 1.1176 1 2 1.27 3 END
CG19  TWO 17X3 +14 AND +15 CLUSTERS, TWO 17X17 CLUSTERS, 4.27
CM X-SEP, Y-SEP
READ PARA TME=200 GEN=160 NPG=1500 NSK=50 NUB=YES XS1=YES
RUN=YES
END PARA
READ GEOM
UNIT 1
 COM=* FUEL PIN *
 CYLINDER  1 1  0.5588 91.44 0.0
 CYLINDER  4 1  0.5588 91.92 0.0
 CYLINDER  5 1  0.5588 91.92 -1.27
 CYLINDER  3 1  0.635  91.92 -1.27
 CYLINDER  4 1  0.635  96.52 -1.27
 CUBOID  2 1  4P.842 96.52 -1.27
UNIT 2
 COM=* WATER CUBOID *
 CUBOID  7 1  4P.842 96.52 -1.27
UNIT 3
 COM=* 17X17 ARRAY OF FUEL PINS *
 ARRAY 1 3R0
UNIT 4
 COM=* 17X3 +14 ROD CLUSTER *
 ARRAY 2 3R0
UNIT 5
 COM=* 17X3 +15 ROD CLUSTER *
 ARRAY 3 3R0
UNIT 6
 COM=* WATER BETWEEN CLUSTERS, 17 RODS WIDE, 4.27 CM THICK
*
 CUBOID  7 1  28.628 0.0 4.27 0.0 96.52 -1.27
UNIT 7
 COM=* LEFT TWO CLUSTERS *
 ARRAY 4 3R0
UNIT 8
 COM=* RIGHT TWO CLUSTERS *
 ARRAY 5 3R0
UNIT 9
 COM=* WATER BETWEEN CLUSTERS, 4.27 CM WIDE *
 CUBOID  7 1  4.27 0.0 39.634 0.0 96.52 -1.27
GLOBAL
UNIT 10
 COM=* ARRAY OF 4 CLUSTERS, 1 IN. ACRYLIC BELOW, WATER
REFLECTOR *
 ARRAY 6 3R0
 REPLICATE 6 1  5R0.0 2.54  1
 REPLICATE 7 1  4R30.0 9.92 15.3  1
END GEOM
READ ARRAY  ARA=1 NUX=17 NUY=17  FILL F1 END FILL
         ARA=2 NUX=17 NUY=4  FILL  65R1 3R2  END FILL
         ARA=3 NUX=17 NUY=4  FILL  51R1 2R2 15R1  END FILL
         ARA=4 NUY=3  FILL 3 6 4 END FILL
         ARA=5 NUY=3  FILL 3 6 5 END FILL
         ARA=6 NUX=3  FILL 7 9 8 END FILL
END ARRAY
READ PLOT
  XUL=0 YUL=.842 ZUL=100 XLR=2.032 YLR=.842
  ZLR=-5  UAX=1  WDN=-1 NAX=20 NDN=50 NCH=' *~ctla~' END
  XUL=-5 YUL=15 ZUL=2 XLR=15 YLR=-5
  ZLR=2   UAX=1  VDN=-1 NAX=120 NDN=100 NCH=' *~ctla~' END
  XUL=-5 YUL=1.016 ZUL=100 XLR=30 YLR=1.016
  ZLR=-6 UAX=1  WDN=-1 NAX=120 NDN=60 NCH=' *~ctla~' END
  PIC=UNIT XUL=-5 YUL=40 ZUL=2 XLR=70 YLR=-5
  ZLR=2 UAX=1 VDN=-1 NAX=60 NDN=60 NCH=' 12345' END
END PLOT
END DATA
END
```

KENO-V.a Input Listing for Case 22 of Table 17 (27-Energy-Group SCALE4 Cross Sections).

```
=CSAS25
C29  CENTER 25X18 CLUSTER, TWO 20X18 CLUSTERS, 6.826 CM SEPARATION
27GROUPNDF4 LATTICECELL
' U(2.35)02
U-234  1 0  2.8563-6 295 END
U-235  1 0  4.8785-4 295 END
U-236  1 0  3.5348-6 295 END
U-238  1 0  2.0009-2 295 END
O  1 0  4.1202-2 295 END
' water
H  2 0  6.6706-2 295 END
O  2 0  3.3353-2 295 END
' 6061 Al (clad)
AL  3 0  5.8433-2 295 END
CR  3 0  6.2310-5 295 END
CU  3 0  6.3731-5 295 END
MG  3 0  6.6651-4 295 END
MN  3 0  2.2115-5 295 END
TI  3 0  2.5375-5 295 END
'       (Zn replaced by Cu)
CU  3 0  3.0967-5 295 END
SI  3 0  3.4607-4 295 END
FE  3 0  1.0152-4 295 END
'  1100 Al (top end plug)
AL  4 0  5.9660-2 295 END
CU  4 0  3.0705-5 295 END
MN  4 0  7.3991-6 295 END
'       (Zn replaced by Cu)
CU  4 0  1.2433-5 295 END
SI  4 0  2.3302-4 295 END
FE  4 0  1.1719-4 295 END
' 5052 Al (lower end plug)
AL  5 0  5.8028-2 295 END
CR  5 0  7.7888-5 295 END
CU  5 0  1.2746-5 295 END
MG  5 0  1.6663-3 295 END
MN  5 0  1.4743-5 295 END
'       (Zn replaced by Cu)
CU  5 0  1.2387-5 295 END
SI  5 0  1.2978-4 295 END
FE  5 0  6.5265-5 295 END
' acrylic
H   6 0  5.6642-2 295 END
C   6 0  3.5648-2 295 END
O   6 0  1.4273-2 295 END
' water
H  7 0  6.6706-2 295 END
O  7 0  3.3353-2 295 END
END COMP
SQUAREPITCH 1.684 1.1176 1 2 1.27 3 END
C29  CENTER 25X18 CLUSTER, TWO 20X18 CLUSTERS, 6.826 CM SEPARATION
READ PARA TME=200 GEN=160 NPG=1500 NSK=50 NUB=YES XS1=YES RUN=YES
END PARA
READ GEOM
UNIT 1
 COM=* FUEL PIN *
 CYLINDER  1 1  0.5588 91.44 0.0
 CYLINDER  4 1  0.5588 91.92 0.0
 CYLINDER  5 1  0.5588 91.92 -1.27
 CYLINDER  3 1  0.635  91.92 -1.27
 CYLINDER  4 1  0.635  96.52 -1.27
 CUBOID  2 1  4P.842 96.52 -1.27
UNIT 2
 COM=* 25X18 ARRAY OF FUEL PINS *
 ARRAY 1 3R0
UNIT 3
 COM=* 20X18 ARRAY OF FUEL PINS *
 ARRAY 2 3R0
UNIT 4
 COM=* WATER BETWEEN CLUSTERS, 6.826 CM WIDE *
 CUBOID  7 1  6.826 0.0 30.312 0.0 96.52 -1.27
GLOBAL
UNIT 5
 COM=* ARRAY OF 3 CLUSTERS, 1 IN. ACRYLIC BELOW, WATER REFLECTOR *
 ARRAY 3 3R0
 REPLICATE 6 1  5R0.0 2.54  1
 REPLICATE 7 1  4R30.0 9.92 15.3  1
END GEOM
READ PLOT
  XUL=-3 YUL=1.016 ZUL=100 XLR=2.032 YLR=1.016
  ZLR=-5  UAX=1  WDN=-1 NAX=30 NDN=110 NCH=' *~ctla~' END
  XUL=-5 YUL=15 ZUL=2 XLR=15 YLR=-5
  ZLR=2   UAX=1  VDN=-1 NAX=120 NCH=' *~ctla~' END
  XUL=-5 YUL=1.016 ZUL=100 XLR=150 YLR=1.016
  ZLR=-6   UAX=1  WDN=-1 NAX=120 NCH=' *~ctla~' END
  PIC=UNIT XUL=-5 YUL=40 ZUL=2 XLR=150 YLR=-5
  ZLR=2   UAX=1  VDN=-1 NAX=120 NCH=' 12345' END
END PLOT
READ ARRAY  ARA=1 NUX=25 NUY=18  FILL F1 END FILL
          ARA=2 NUX=20 NUY=18  FILL F1 END FILL
          ARA=3 NUX=5  FILL 3 4 2 4 3 END FILL
END ARRAY
END DATA
END
```

A.2 MCNP Input Listings

Version 4XD of MCNP was used.

Fuel rod clusters were created by filling cuboids with a universe containing an infinite lattice of fuel rods.

MCNP k_{eff} calculations used 110 generations of 1500 neutrons each after skipping 50 generations.

MCNP Input Listing for Case 3 of Table 16.

```
M11  23X22 CLUSTER + 17 RODS, U(2.35)O2 RODS, 1.684 CM PITCH
1     1 .06170524 -1 7 -8 u=1 imp:n=1 $ uo2 fuel
2     3 .0597516   1 -2 -9 u=1 imp:n=1 $ clad
3     4 .06006075  -1 8 -9 u=1 imp:n=1 $ top end plug (lower piece)
4     4 .06006075  -2 9 u=1 imp:n=1 $ top end plug (top piece)
5     5 .06000711  -1 -7 u=1 imp:n=1 $ lower end plug
6     2 .100059  2 u=1 imp:n=1 $ water
7     0  -4 3 -6 5  imp:n=1 lat=1 u=2 fill=1  $ lattice of fuel rods
8     0 -10 11 -20 21 -22 23 fill=2 imp:n=1  $ rod cluster
9     0 -12 11 -13 20 -22 23 fill=2 imp:n=1  $ partial row
10    2 .100059  12 -10 -13 20 -22 23  imp:n=1 $ water of partial row
11    6 .106563  -23 29 -10 11 -13 21 imp:n=1  $ acrylic support plate
12    2 .100059 (-11:10:13:-21:22:-29) -24 25 -26 27 -28 30 imp:n=1 $ water
13    0  24:-25:26:-27:28:-30  imp:n=0

1     c/z .842 .842 .5588  $ fuel cylinder
2     c/z .842 .842 .635  $ clad cylinder
3     px  0.0  $ fuel rod cell boundary
4     px  1.684  $ fuel rod cell boundary
5     py  0.0  $ fuel rod cell boundary
6     py  1.684  $ fuel rod cell boundary
7     pz  0.0  $ bottom of fuel
8     pz  91.44  $ top of fuel
9     pz  91.92  $ top of clad
10    px  38.7319  $ farthest side of cluster  !!
11    px  .0001  $ closest side of cluster
12    px  28.6279  $ division between rods and water of partial row !!
13    py  38.7319  $ farthest side of partial row  !!
20    py  37.0479  $ side of complete cluster  !!
21    py  .0001  $ side of cluster
22    pz  96.52  $ top of fuel rod
23    pz  -1.27  $ bottom of fuel rod
24    px  68.732  $ side of water reflector  !!
25    px  -30  $ side of water reflector
26    py  68.732  $ side of water reflector  !!
27    py  -30  $ side of water reflector
28    pz  106.44  $ top of water
29    pz  -3.81  $ bottom of acrylic support plate
30    pz  -19.11  $ bottom of water

kcode  1500 1 50 160 50000
c     kcode  100 1 1 5 50000
sdef  x=d1 y=d2 z=d3 cel=d4
si1   0 70
sp1   0 1
si2   0 70
sp2   0 1
si3   0 100
sp3   0 1
si4   l 8 9
sp4   v
print
c     m1 is UO2 fuel
m1    92234.50c 2.8563e-6 92235.50c 4.8785e-4
      92236.50c 3.5348e-6 92238.50c 2.0009e-2
      8016.50c  4.1202e-2
c     m2 is water with 10.4 mg/liter Gd
m2    8016.50c 3.3353e-2  1001.50c 6.6706e-2
      64152.50c 7.9656e-11  64154.50c 8.6825e-10
      64155.50c 5.8946e-9  64156.50c 8.1528e-9
      64157.50c 6.2331e-9  64158.50c 9.8933e-9
      64160.50c 8.7064e-9
```

MCNP Input Listing for Case 3 of Table 16 (cont'd).

```
mt2   lwtr.01t
c     m3 is 6061 Al (clad)
m3    13027.50c  5.8433e-2  24000.50c  6.2310e-5
      29000.50c  6.3731e-5  12000.50c  6.6651e-4
      25055.50c  2.2115e-5  22000.50c  2.5375e-5
c     Zn replaced by Cu, below
      29000.50c  3.0967e-5  14000.50c  3.4607e-4
      26000.50c  1.0152e-4
c     m4 is 1100 aluminum (top end plug)
m4    13027.50c  5.9660e-2  29000.50c  3.0705e-5
      25055.50c  7.3991e-6
c       Zn replaced by Cu, below
      29000.50c  1.2433e-5  14000.50c  2.3302e-4
      26000.50c  1.1719e-4
c     m5 is 5052 aluminum (lower end plug)
m5    13027.50c  5.8028e-2  24000.50c  7.7888e-5
      29000.50c  1.2746e-5  12000.50c  1.6663e-3
      25055.50c  1.4743e-5
c       Zn replaced by Cu, below
      29000.50c  1.2387e-5  14000.50c  1.2978e-4
      26000.50c  6.5265e-5
c     m6 is acrylic (support plate)
m6    1001.50c 5.6642e-2  6000.50c 3.5648e-2
      8016.50c 1.4273e-2
mt6   poly.01t
```

MCNP Input Listing for Case 10 of Table 16.

```
 M18 ONE 17X17+4 CLSTR, ONE 17x17+5 CLSTR OF U(2.35)O2 RODS, 1.68 CM X-SEP
1    1 .06170524 -1 7 -8 u=1 imp:n=1 $ uo2 fuel
2    3 .0597516   1 -2 -9 u=1 imp:n=1 $ clad
3    4 .06006075  -1 8 -9 u=1 imp:n=1 $ top end plug (lower piece)
4    4 .06006075  -2 9 u=1 imp:n=1 $ top end plug (top piece)
5    5 .06000711  -1 -7 u=1 imp:n=1 $ lower end plug
6    2 .100059  2 u=1 imp:n=1 $ water
7    0  -4 3 -6 5  imp:n=1 lat=1 u=2 fill=1  $ lattice of fuel rods
8    0 -11 10 -21 20 -33 34 fill=2 imp:n=1  $ first rod cluster
9    0 -15 14 -21 20 -33 34 fill=2(30.308 0 0) imp:n=1  $ second rod cluster
10   0  -13 10 -25 21 -33 34 fill=2 imp:n=1  $ left partial row
11   2 .100059  13 -11 -25 21 -33 34 imp:n=1 $ water of left partial row
12   2 .100059  -16 14 -25 21 -33 34 imp:n=1 $ water of right partial row
13   0 16 -15 -25 21 -33 34 fill=2(30.308 0 0) imp:n=1  $ right partial row
14   6 .106563  -34 35 -15 10 -25 20 imp:n=1  $ acrylic support plate
15   2 .100059 -14 11 -25 20 -33 34 imp:n=1  $ water between clusters
16   2 .100059 (-10:15:25:-20:33:-35) 41 -40 -42 43 -44 45 imp:n=1 $ water
17   0  -41:40:42:-43:44:-45 imp:n=0

1    c/z .842 .842 .5588  $ fuel cylinder
2    c/z .842 .842 .635  $ clad cylinder
3    px  0.0  $ fuel rod cell boundary
4    px  1.684  $ fuel rod cell boundary
5    py  0.0  $ fuel rod cell boundary
6    py  1.684  $ fuel rod cell boundary
7    pz  0.0  $ bottom of fuel
8    pz  91.44  $ top of fuel
9    pz  91.92  $ top of clad
10   px  .0001  $ closest x-edge of closest cluster
11   px  28.6279  $ farthest x-edge of closest cluster
13   px  6.7359  $ division between rods and water in left partial row
14   px  30.3081  $ closest x-edge of farthest cluster
15   px  58.9359  $ farthest x-edge of farthest cluster
16   px  50.5161  $ division between water and rods in right partial row
20   py  .0001  $ closest y-edge of closest clusters
21   py  28.6279  $ farthest y-edge of full clusters
25   py  30.3119  $ farthest y-edge of partial rows
33   pz  96.52  $ top of fuel rod
34   pz  -1.27  $ bottom of fuel rod
35   pz  -3.81  $ bottom of acrylic support plate
40   px  88.936  $ side of water reflector
41   px  -30  $ side of water reflector
42   py  60.312  $ side of water reflector
43   py  -30  $ side of water reflector
44   pz  106.44  $ top of water
45   pz  -19.11  $ bottom of water

kcode  1500 1 50 160 50000
sdef  x=d1 y=d2 z=d3 cel=d4
si1   0 29
sp1   0 1
si2   0 100
sp2   0 1
si3   0 100
sp3   0 1
si4   l 8
sp4   v
print
c     m1 is U(2.35)O2 fuel
m1    92234.50c 2.8563e-6 92235.50c 4.8785e-4
      92236.50c 3.5348e-6 92238.50c 2.0009e-2
      8016.50c  4.1202e-2
```

MCNP Input Listing for Case 10 of Table 16 (cont'd).

```
c     m2 is water with 10.4 mg/liter Gd
m2    8016.50c 3.3353e-2  1001.50c 6.6706e-2
      64152.50c 7.9656e-11  64154.50c 8.6825e-10
      64155.50c 5.8946e-9  64156.50c 8.1528e-9
      64157.50c 6.2331e-9  64158.50c 9.8933e-9
      64160.50c 8.7064e-9
mt2   lwtr.01t
c     m3 is 6061 Al (clad)
m3    13027.50c  5.8433e-2  24000.50c  6.2310e-5
      29000.50c  6.3731e-5  12000.50c  6.6651e-4
      25055.50c  2.2115e-5  22000.50c  2.5375e-5
c     Zn replaced by Cu, below
      29000.50c  3.0967e-5  14000.50c  3.4607e-4
      26000.50c  1.0152e-4
c     m4 is 1100 aluminum (top end plug)
m4    13027.50c  5.9660e-2  29000.50c  3.0705e-5
      25055.50c  7.3991e-6
c       Zn replaced by Cu, below
      29000.50c  1.2433e-5  14000.50c  2.3302e-4
      26000.50c  1.1719e-4
c     m5 is 5052 aluminum (lower end plug)
m5    13027.50c  5.8028e-2  24000.50c  7.7888e-5
      29000.50c  1.2746e-5  12000.50c  1.6663e-3
      25055.50c  1.4743e-5
c       Zn replaced by Cu, below
      29000.50c  1.2387e-5  14000.50c  1.2978e-4
      26000.50c  6.5265e-5
c     m6 is acrylic (support plate)
m6    1001.50c 5.6642e-2  6000.50c 3.5648e-2
      8016.50c 1.4273e-2
mt6   poly.01t
```

MCNP Input Listing for Case 11 of Table 16.

```
M19 17X3+14, 17X3+15, AND TWO 17X17 CLSTRS OF U(2.35)O2 RODS, 4.27 CM SEPS
1    1 .06170524 -1 7 -8 u=1 imp:n=1 $ uo2 fuel
2    3 .0597516   1 -2 -9 u=1 imp:n=1 $ clad
3    4 .06006075  -1 8 -9 u=1 imp:n=1 $ top end plug (lower piece)
4    4 .06006075  -2 9 u=1 imp:n=1 $ top end plug (top piece)
5    5 .06000711  -1 -7 u=1 imp:n=1 $ lower end plug
6    2 .100059  2 u=1 imp:n=1 $ water
7    0  -4 3 -6 5  imp:n=1 lat=1 u=2 fill=1  $ lattice of fuel rods
8    0 -11 10 -21 20 -33 34 fill=2 imp:n=1  $ first rod cluster
9    0 -15 14 -21 20 -33 34 fill=2(32.898 0 0) imp:n=1  $ second rod cluster
10   0 -11 10 -25 24 -33 34 fill=2(0 32.898 0)  imp:n=1  $ third rod cluster
11   0 -15 14 -25 24 -33 34 fill=2(32.898 32.898 0)  imp:n=1  $ fourth rod cluster
12   0  -13 10 -26 25 -33 34 fill=2(0 32.898 0) imp:n=1  $ left partial row
13   0  16 -15 -26 25 -33 34 fill=2(32.898 32.898 0) imp:n=1  $ right partial row
14   2 .100059  -11 13 -26 25 -33 34 imp:n=1 $ water of left partial row
15   2 .100059  -16 14 -26 25 -33 34 imp:n=1 $ water of right partial row
16   6 .106563  -34 35 -15 10 -26 20 imp:n=1  $ acrylic support plate
17   2 .100059 -14 11 -26 20 -33 34 imp:n=1  $ water between clusters
18   2 .100059 -11 10 -24 21 -33 34 imp:n=1  $ water between clusters
19   2 .100059 -15 14 -24 21 -33 34 imp:n=1  $ water between clusters
20   2 .100059 (-10:15:26:-20:33:-35) 41 -40 -42 43 -44 45 imp:n=1 $ water
21   0  -41:40:42:-43:44:-45 imp:n=0

1    c/z .842 .842 .5588  $ fuel cylinder
2    c/z .842 .842 .635  $ clad cylinder
3    px  0.0  $ fuel rod cell boundary
4    px  1.684  $ fuel rod cell boundary
5    py  0.0  $ fuel rod cell boundary
6    py  1.684  $ fuel rod cell boundary
7    pz  0.0  $ bottom of fuel
8    pz  91.44  $ top of fuel
9    pz  91.92  $ top of clad
10   px  .0001  $ closest x-edge of closest cluster
11   px  28.6279  $ farthest x-edge of closest cluster
13   px  23.5759  $ division between rods and water in left partial row
14   px  32.8981  $ closest x-edge of farthest cluster
15   px  61.5259  $ farthest x-edge of farthest cluster
16   px  36.2661  $ division between rods and water in right partial row
20   py  .0001  $ closest y-edge of closest clusters
21   py  28.6279  $ farthest y-edge of closest clusters
24   py  32.8981  $ closest y-edge of farthest clusters **
25   py  37.9499  $ farthest y-edge of farthest complete cluster
26   py  39.6339  $ farthest y-edge of partial row
33   pz  96.52  $ top of fuel rod
34   pz  -1.27  $ bottom of fuel rod
35   pz  -3.81  $ bottom of acrylic support plate
40   px  91.526  $ side of water reflector
41   px  -30  $ side of water reflector
42   py  69.634  $ side of water reflector
43   py  -30  $ side of water reflector
44   pz  106.44  $ top of water
45   pz  -19.11  $ bottom of water

kcode  1500 1 50 160 50000
sdef  x=d1 y=d2 z=d3 cel=d4
si1   0 62
sp1   0 1
si2   0 40
sp2   0 1
si3   0 92
sp3   0 1
si4   l 8 9 10 11
```

MCNP Input Listing for Case 11 of Table 16 (cont'd).

```
sp4   v
print
c     m1 is U(2.35)O2 fuel
m1    92234.50c 2.8563e-6 92235.50c 4.8785e-4
      92236.50c 3.5348e-6 92238.50c 2.0009e-2
      8016.50c  4.1202e-2
c     m2 is water with 10.4 mg/liter Gd
m2    8016.50c 3.3353e-2  1001.50c 6.6706e-2
      64152.50c 7.9656e-11  64154.50c 8.6825e-10
      64155.50c 5.8946e-9  64156.50c 8.1528e-9
      64157.50c 6.2331e-9  64158.50c 9.8933e-9
      64160.50c 8.7064e-9
mt2   lwtr.01t
c     m3 is 6061 Al (clad)
m3    13027.50c  5.8433e-2  24000.50c  6.2310e-5
      29000.50c  6.3731e-5  12000.50c  6.6651e-4
      25055.50c  2.2115e-5  22000.50c  2.5375e-5
c     Zn replaced by Cu, below
      29000.50c  3.0967e-5  14000.50c  3.4607e-4
      26000.50c  1.0152e-4
c     m4 is 1100 aluminum (top end plug)
m4    13027.50c  5.9660e-2  29000.50c  3.0705e-5
      25055.50c  7.3991e-6
c       Zn replaced by Cu, below
      29000.50c  1.2433e-5  14000.50c  2.3302e-4
      26000.50c  1.1719e-4
c     m5 is 5052 aluminum (lower end plug)
m5    13027.50c  5.8028e-2  24000.50c  7.7888e-5
      29000.50c  1.2746e-5  12000.50c  1.6663e-3
      25055.50c  1.4743e-5
c       Zn replaced by Cu, below
      29000.50c  1.2387e-5  14000.50c  1.2978e-4
      26000.50c  6.5265e-5
c     m6 is acrylic (support plate)
m6    1001.50c 5.6642e-2  6000.50c 3.5648e-2
      8016.50c 1.4273e-2
mt6   poly.01t
```

MCNP Input Listing for Case 22 of Table 17.

```
M29  TWO 20X18 CLUSTERS, ONE 25X18 OF U(2.35)O2 RODS, 6.826 CM SEPR
1     1 .06170524 -1 7 -8 u=1 imp:n=1 $ uo2 fuel
2     3 .0597516   1 -2 -9 u=1 imp:n=1 $ clad
3     4 .06006075  -1 8 -9 u=1 imp:n=1 $ top end plug (lower piece)
4     4 .06006075  -2 9 u=1 imp:n=1 $ top end plug (top piece)
5     5 .06000711  -1 -7 u=1 imp:n=1 $ lower end plug
6     2 .100059  2 u=1 imp:n=1 $ water
7     0  -4 3 -6 5  imp:n=1 lat=1 u=2 fill=1  $ lattice of fuel rods
8     0 -10 11 -20 21 -22 23 fill=2 imp:n=1  $ first rod cluster
9     0 -13 12 -20 21 -22 23 fill=2(40.506 0 0) imp:n=1  $ second rod cluster
10    0 -15 14 -20 21 -22 23 fill=2(89.432 0 0) imp:n=1  $ third rod cluster
11    6 .106563  -23 29 -15 11 -20 21 imp:n=1  $ acrylic support plate
12    2 .100059 -12 10 -20 21 -22 23 imp:n=1  $ water between clusters
13    2 .100059 -14 13 -20 21 -22 23 imp:n=1  $ water between clusters
14    2 .100059 (-11:15:20:-21:22:-29) -24 25 -26 27 -28 30 imp:n=1 $ water
15    0  24:-25:26:-27:28:-30  imp:n=0

1     c/z .842 .842 .5588  $ fuel cylinder
2     c/z .842 .842 .635  $ clad cylinder
3     px  0.0  $ fuel rod cell boundary
4     px  1.684  $ fuel rod cell boundary
5     py  0.0  $ fuel rod cell boundary
6     py  1.684  $ fuel rod cell boundary
7     pz  0.0  $ bottom of fuel
8     pz  91.44  $ top of fuel
9     pz  91.92  $ top of clad
10    px  33.6799  $ farthest edge of closest cluster
11    px  .0001  $ closest edge of closest cluster
12    px  40.5061  $ closest edge of center cluster **
13    px  82.6059  $ farthest edge of center cluster
14    px  89.4321  $ closest edge of farthest cluster **
15    px  123.1119  $ farthest end of clusters
20    py  30.3119  $ sides of clusters
21    py  .0001  $ sides of clusters
22    pz  96.52  $ top of fuel rod
23    pz  -1.27  $ bottom of fuel rod
24    px  153.112  $ side of water reflector
25    px  -30  $ side of water reflector
26    py  60.312  $ side of water reflector
27    py  -30  $ side of water reflector
28    pz  106.44  $ top of water
29    pz  -3.81  $ bottom of acrylic support plate
30    pz  -19.11  $ bottom of water

kcode  1500 1 50 160 50000
c     kcode  100 1 1 5 50000
sdef  x=d1 y=d2 z=d3 cel=d4
si1   0 200
sp1   0 1
si2   0 100
sp2   0 1
si3   0 100
sp3   0 1
si4   l 8 9 10
sp4   v
print
c     m1 is UO2 fuel
m1    92234.50c 2.8563e-6 92235.50c 4.8785e-4
      92236.50c 3.5348e-6 92238.50c 2.0009e-2
      8016.50c  4.1202e-2
c     m2 is water
m2    8016.50c 3.3353e-2  1001.50c 6.6706e-2
```

MCNP Input Listing for Case 22 of Table 17 (cont'd).

```
mt2   lwtr.01t
c     m3 is 6061 Al (clad)
m3    13027.50c  5.8433e-2  24000.50c  6.2310e-5
      29000.50c  6.3731e-5  12000.50c  6.6651e-4
      25055.50c  2.2115e-5  22000.50c  2.5375e-5
c     Zn replaced by Cu, below
      29000.50c  3.0967e-5  14000.50c  3.4607e-4
      26000.50c  1.0152e-4
c     m4 is 1100 aluminum (top end plug)
m4    13027.50c  5.9660e-2  29000.50c  3.0705e-5
      25055.50c  7.3991e-6
c       Zn replaced by Cu, below
      29000.50c  1.2433e-5  14000.50c  2.3302e-4
      26000.50c  1.1719e-4
c     m5 is 5052 aluminum (lower end plug)
m5    13027.50c  5.8028e-2  24000.50c  7.7888e-5
      29000.50c  1.2746e-5  12000.50c  1.6663e-3
      25055.50c  1.4743e-5
c       Zn replaced by Cu, below
      29000.50c  1.2387e-5  14000.50c  1.2978e-4
      26000.50c  6.5265e-5
c     m6 is acrylic (support plate)
m6    1001.50c 5.6642e-2  6000.50c 3.5648e-2
      8016.50c 1.4273e-2
mt6   poly.01t
```

A.3 ONEDANT/TWODANT Input Listings

Because of the heterogeneity of the fuel rod lattice, neither ONEDANT nor TWODANT calculations were performed.

APPENDIX B: CORRELATION BETWEEN CASE NUMBER AND ORIGINAL EXPERIMENT NUMBER

Table B.1 correlates the experiment "Case" number, as used in this evaluation, with the original experiment number. Logbooks are stored at the Los Alamos National Laboratory Archives under the original experiment number. (Logbooks for all experiments below were listed on the inventory for the shipment from Hanford to Los Alamos as being in Box 11, except for one configuration for Case 21 and for Case 22, which were in Box 6.)

Table B.1. Correlation of Case Number with Original Experiment Number.

Case Number	Original Experiment Number
1	SSC-2.35-000-105
2	SSC-2.35-000-094
3	SSC-2.35-000-096
4	SSC-2.35-000-095
5	SSC-2.35-000-106
6	SSC-2.35-000-097
7	SSC-2.35-000-099
8	SSC-2.35-000-098
9	SSC-2.35-000-069
10	SSC-2.35-000-108
11	SSC-2.35-000-070
12	SSC-2.35-000-071
13	SSC-2.35-000-078
14	SSC-2.35-000-077
15	SSC-2.35-000-076
16	SSC-2.35-000-075
17	SSC-2.35-000-074
18	SSC-2.35-000-073
19	SSC-2.35-000-072
20	SSC-2.35-000-112
21, 22	SSC-2.35-000-120 SSC-2.35-000-(149-157)
23	SSC-2.35-000-(149-157)

APPENDIX C: EFFECT OF WATER IMPURITIES ON k_{eff}

Results of analyses of water impurities from References 1-10 are given in Table C.1.

Note that two sets of results from Reference 8, the gadolinium-water experiments, are given. Two separate analyses, one of the gadolinium solution and the other of the gadolinium nitrate powder, were done. The first set of values is the largest amount of impurity found in any solution sample used in an approach to critical experiment (Reference 8, p. C.4). The second set of values is from the gadolinium nitrate powder analysis and is based on the highest gadolinium concentration used, which was 1.481 g Gd/liter (0.00148 g Gd/cm^3). Shaded concentrations are maximum values.

Concentrations of impurities in solution from their weight percent in gadolinium nitrate powder were calculated in the following manner: The molecular formula for the gadolinium nitrate powder is given as $Gd(NO_3)_3 \times 4.91\ H_2O$, giving a molecular weight of 431.72. Therefore, assuming a solution concentration of 1.481 g Gd/liter, the concentration of the impurity in solution from the given weight percent of the impurity in the gadolinium nitrate powder (Reference 8, p. C.3) is:

$$0.001481\frac{g}{cm^3}\ \frac{(wt.\%\ impurity)}{(wt.\%\ Gd)} = \frac{.001481\frac{g}{cm^3}(wt.\%\ impurity)}{[100 - \sum(wt.\%\ impurities)]\frac{A_{W,Gd}}{M_{W,Gd\ powder}}}$$

$$= \frac{0.001481\frac{g}{cm^3}(wt.\%\ impurity)}{[100 - 0.4735]\frac{157.25}{431.72}} = 4.08534 \times 10^{-5}(wt.\%\ impurity)\frac{g}{cm^3}$$

Table C.1. Impurity Components of Water (g/m^3).[a] (Maximum values are shaded.)

Reference→ Component↓	1, p. 8[b]	2 (p. 6) and 3 (p. 7)[c]	4 (p. 8)[c]	5 (p. 9); 6 (p. 7); 7 (p. 6)[d]	8 (p. C.4)	8 (p. C.3)	9 (p. B.2)[e]	10 (p. B.2)
Cl	26.2±5.4	30.2±5.8	1.7±.6	≤ 5	-	-	11	18
NO_3^-	0.24±.12	0.42±.16	0.02±.01	0.02	-	-	<0.38[f]	2.83[f]
Cr	<0.028	<0.01	<0.01	<0.01	-	0.041	<0.01	<0.005
Zn	0.35±.05	0.26±.07	0.9±1.1	16	10.6	0.0613	<0.05	0.32
Mn	<0.55	<0.01	<0.01	<0.01	-	0.041	<0.01	<0.01
Pb	<0.015	<0.005	0.008±.001	<0.005	2.1	1.0220	<0.002	<0.005
F	0.21±.02	0.15±.04	0.15±.04	0.18	-	-	0.12	0.12
Fe	<0.06	<0.03	<0.03	24	-	0.21	0.12	0.20
Cu	<0.06	<0.01	<0.01	<0.01	18.2	0.123	<0.05	<0.05
Cd	0.004±.001	0.006±.001	0.020±.006	0.001	-	0.041	0.002	0.0006
Gd	-	-	10.4±3.6	-	-	-	-	<10
SO_3	6.7±.4	6.6±.04	13.4±5.0	14.5	-	-	21	16
$CaCO_3$	-	-	-	-	19.2[g]	1.02[g]	51.2	35
B	-	-	-	-	0.09	1.02	-	<25
Al	-	-	-	-	7.3	2.04	-	-
Eu	-	-	-	-	0.08	1.23	-	-
Mg	-	-	-	-	5.7	0.204	-	-
Nd	-	-	-	-	12.2	2.04	-	-
Si	-	-	-	-	3.1	2.04	-	-
Ni	-	-	-	-	6.8	0.204	-	-
Y	-	-	-	-	0.17	0.41	-	-

Reference→ Component↓	1, p. 8[b]	2 (p. 6) and 3 (p. 7)[c]	4 (p. 8)[c]	5 (p. 9); 6 (p. 7); 7 (p. 6)[d]	8 (p. C.4)	8 (p. C.3)	9 (p. B.2)[e]	10 (p. B.2)
Others	-	-	-	-	Nb 0.3	Ag .041 Au .041 Ba .041 Be 2.04 Ce .102 Co .041 Dy .204 Hf .041 K .204 Li .041 La .204 Mo .041 Na 1.02 Pt .204 Rh .102 Ru 1.02 Sm .204 Sn 1.02 Sr .041 Tb .204 Ti 2.04 U .204 V .041 W .102 Zr .041	-	-
Dissolved Solids (g/m^3)	-	137±5	113±28	61 ± 3	-	-	109	83

(a) If one cubic centimeter has a mass of 1 gram, then this is the same as PPM (parts per million) by weight.
(b) Average of samples taken at the beginning and near the end of the experiments.
(c) Error limits are standard deviations observed in three samples.
(d) In Reference 7, analysis is prior to boron additions (Reference 7, p. 2).
(e) Largest values of three samples.
(f) "Nitrate (as N) mg/liter."
(g) As Ca.

Effect Due to Water Density Reduction - The maximum amount of dissolved solids reported was 137 grams per cubic meter of solution. Assume that the dissolved solids at a concentration of 200 g/m^3, have the same density as water (~1 g/cm^3), and displace the water. These are conservative assumptions since the 200 g/m^3 concentration is greater than any measured total impurity concentration and since many materials are denser than water and, when dissolved in water, do not displace as much water as their dry volume. The percentage of water volume displaced by the solute is then $200/10^6 \times 100 = 0.02\%$. To see the effect of reduced water density, the water volume fraction is reduced by this percentage. The resulting change in k_{eff} of this conservative approximation is less than 0.04%.[a] Therefore, the effect on k_{eff} of water density reduction due to impurities is negligible.

Effect Due to Presence of Individual Impurities - Listed in Table C.2 are the percent changes in k_{eff} for the addition of the maximum measured amounts of each impurity, as calculated by ONEDANT, using the 27-group cross sections processed by CSASIX.[b] No changes are greater than 0.005% except those from boron and gadolinium impurities, with Δk_{eff} values of 0.9% and 1.7%, respectively. Therefore, critical configurations from the two references with these maximal possible impurity concentrations, References 4 and 10, should include these two impurities in the water.

Because no experiments from Reference 10 are included in this evaluation, only the gadolinium impurity reported in Reference 4 must be included in the water moderator/reflector in models of experiments from Reference 4 (Cases 1-21).

[a] This is based on ONEDANT calculations of $U(2.35)O_2$ fuel rods in a cylindrical, water-reflected, near-optimal square-pitched array, using 27-group cross sections created by CSASIX.

[b] Because zinc and platinum were not in the Standard Composition Library for CSAS, copper was substituted for zinc and gold was substituted for platinum. (Copper and gold total cross sections appear to be similar, conservative substitutes for zinc and platinum.)

Table C.2. Calculated Effect of Impurities on Δk_{eff}.

Impurity	Concentration (g/cm^3)	Atom Density (atoms/barn-cm)	% Δk_{eff}
Ag	4.09×10^{-08}	2.281×10^{-10}	0
Al	7.30×10^{-06}	1.629×10^{-07}	0
Au	4.09×10^{-08}	1.249×10^{-10}	0
B	2.50×10^{-05}	1.393×10^{-06}	-0.885 -0.784[(a)]
	1.02×10^{-06}[(b)]	5.682×10^{-08}	-0.009
Ba	4.09×10^{-08}	1.791×10^{-10}	0
Be	2.04×10^{-06}	1.365×10^{-07}	0.002
$CaCO_3$	5.12×10^{-05}	3.081×10^{-07}	0.005
Cd	4.09×10^{-08}	2.189×10^{-10}	0
Ce	1.02×10^{-07}	4.390×10^{-10}	0.001
Cl	3.60×10^{-05}	6.115×10^{-07}	0.004
Co	4.09×10^{-08}	4.175×10^{-10}	0
Cr	4.09×10^{-08}	4.732×10^{-10}	0
Cu	1.82×10^{-05}	1.725×10^{-07}	0.002
Eu	1.22×10^{-06}	4.838×10^{-09}	-0.005
F	2.30×10^{-07}	7.291×10^{-09}	0
Fe	2.40×10^{-05}	2.588×10^{-07}	0.003
Gd	1.40×10^{-05}	5.361×10^{-08}	-1.653 -1.830[(a)]
	1.00×10^{-05}[(c)]	3.830×10^{-08}	-1.200
	5.00×10^{-06}[(d)]	1.915×10^{-08}	-0.592
Hf	4.09×10^{-08}	1.378×10^{-10}	0
K	2.04×10^{-07}	3.146×10^{-09}	0
Li	4.09×10^{-08}	3.544×10^{-09}	0
La	2.04×10^{-07}	8.856×10^{-10}	0
Mg	5.70×10^{-06}	1.412×10^{-07}	0
Mn	5.50×10^{-07}	6.029×10^{-09}	0.002
Mo	4.09×10^{-08}	2.564×10^{-10}	0

Impurity	Concentration (g/cm^3)	Atom Density (atoms/barn-cm)	% Δk_{eff}
N	$2.83x10^{-06}$	$1.217x10^{-07}$	0.002
Na	$1.02x10^{-06}$	$2.675x10^{-08}$	0.002
Nb	$3.00x10^{-07}$	$1.945x10^{-09}$	0
Nd	$1.22x10^{-05}$	$5.094x10^{-08}$	0.001
Ni	$6.80x10^{-06}$	$6.977x10^{-08}$	0.002
Pb	$2.10x10^{-06}$	$6.103x10^{-09}$	0
Pt[(e)]	$2.04x10^{-07}$	$6.305x10^{-10}$	0
Rh	$1.02x10^{-07}$	$5.977x10^{-10}$	0.001
Ru	$1.02x10^{-06}$	$6.085x10^{-09}$	0.001
Si	$3.10x10^{-06}$	$6.647x10^{-08}$	0
Sm	$2.04x10^{-07}$	$8.179x10^{-10}$	0.001
Sn	$1.02x10^{-06}$	$5.182x10^{-09}$	0
SO_3	$1.84x10^{-05}$	$1.384x10^{-07}$	0.002
Sr	$4.09x10^{-08}$	$2.808x10^{-10}$	0.001
Tb	$2.03x10^{-07}$	$7.709x10^{-10}$	0.001
Ti	$2.04x10^{-06}$	$2.568x10^{-08}$	0
U	$2.04x10^{-07}$	$5.168x10^{-10}$	0
V	$4.09x10^{-08}$	$4.830x10^{-10}$	0
W	$1.02x10^{-07}$	$3.345x10^{-10}$	0
Y	$4.09x10^{-07}$	$2.767x10^{-09}$	0
Zn[(f)]	$1.60x10^{-05}$	$1.474x10^{-07}$	0.003
Zr	$4.09x10^{-08}$	$2.697x10^{-10}$	0

(a) MCNP calculation.
(b) This is an actual measured value, from Reference 8.
(c) Measured maximum value from Reference 10.
(d) Half of measured maximum value from Reference 10.
(e) Because platinum was not in the cross-section library, gold was substituted.
(f) Because zinc was not in the cross-section library, copper was substituted.

APPENDIX D:SAMPLE CSASIX AND ONEDANT INPUTS FOR SENSITIVITY STUDIES USING HOMOGENIZED FUEL ROD REGION

```
=CSASIX
GENERATE 27-GRP LIB FOR 2.35 WT% UO2 PNL FUEL PINS IN WATER
27GROUPNDF4 LATTICECELL
U-234  1 0  2.85626-6 291 END
U-235  1 0  4.87852-4 291 END
U-236  1 0  3.53484-6 291 END
U-238  1 0  2.00094-2 291 END
O  1 0  4.12021-2 291 END
H  2 0  6.67619-2 291 END
O  2 0  3.33809-2 291 END
Al  3 0  6.01507-2 291 END
H  4 0  6.67619-2 291 END
O  4 0  3.33809-2 291 END
END COMP
SQUAREPITCH 2.032 1.1176 1 2 1.27 3 END
END


    1     0     0
SLAB OF U(2.35)O2 FUEL PINS IN WATER, BASE CASE
/  Block 1
igeom=slab ngroup=27 isn=16 niso=5 mt=5 nzone=5 im=4 it=251  T

/  Block 2
xmesh= 0 44.72 45.72 46.72 60.72
xints= 179    8     8     56
zones=   5    5     4      4 T

/  Block 3
lib=xs27.p3
chivec= .021 .188 .215 .125 .166 .180 .090 .014 .001 18z
maxord=3 ihm=42 iht=3 ihs=16 ititl=1 ifido=2 i2lp1=1
T

/ Block 4
matls=isos  assign=matls  T

/  Block 5
ievt=1 isct=3 ibl=1 ibr=0 epsi=.000001  T

/  Block 6
pted=0 zned=1  T
```